NOAA Technical Report NESDIS 106

CALIBRATION OF THE ADVANCED MICROWAVE SOUNDING UNIT-A RADIOMETERS FOR NOAA-N AND NOAA-N'

Washington, D.C.
September 2002

U.S. DEPARTMENT OF COMMERCE
National Oceanic and Atmospheric Administration
National Environmental Satellite, Data, and Information Service

NOAA TECHNICAL REPORTS

National Environmental Satellite, Data, and Information Service

The National Environmental Satellite, Data, and Information Service (NESDIS) manages the Nation's civil Earth-observing satellite systems, as well as global national data bases for meteorology, oceanography, geophysics, and solar-terrestrial sciences. From these sources, it develops and disseminates environmental data and information products critical to the protection of life and property, national defense, the national economy, energy development and distribution, global food supplies, and the development of natural resources.

Publication in the NOAA Technical Report series does not preclude later publication in scientific journals in expanded or modified form. The NESDIS series of NOAA Technical Reports is a continuation of the former NESS and EDIS series of NOAA Technical Reports and the NESC and EDS series of Environmental Science Services Administration (ESSA) Technical Reports.

A limited number of copies are available by contacting Jessica Pejsa, NOAA/NESDIS, E/RA2, 5200 Auth Road, Room 601, Camp Springs, Maryland 20746, (301) 763-8282. Copies can also be ordered from the National Technical Information Service (NTIS), U.S. Department of Commerce, Sills Bldg., 5285 Port Royal Road, Springfield, VA 22161, (703) 487-4650 (prices on request for paper copies or microfiche, please refer to PB number when ordering). A partial listing of more recent reports appear below:

NESDIS 67 The Relationship between Water Vapor Plumes and Extreme Rainfall Events during the Summer Season. Wassila Thiao, Roderick A. Scofield and Jacob Robinson, May 1993.

NESDIS 68 AMSU-A Engineering Model Calibration. Tsan Mo, Michael P. Weinreb, Norman C. Grody and David Q. Wark, June 1993.

NESDIS 69 Nonlinearity Corrections for the Thermal Infrared Channels of the Advanced Very High Resolution Radiometer: Assessment and Recommendations. C.R. N. Rao (Editor), June 1993.

NESDIS 70 Degradation of the Visible and Near-Infrared Channels of the Advanced Very High Resolution Radiometer on the NOAA-9 Spacecraft: Assessment and Recommendations for Corrections. C.R. N. Rao (Editor), June 1993.

NESDIS 71 Spectral Radiance-Temperature Conversions for Measurements by AVHRR Thermal Channels 3,4,5. Paul A. Davis, August 1993.

NESDIS 72 Summary of the NOAA/NESDIS Workshop on Development of a Global Satellite/in Situ Environmental Database. Edited by K.P. Gallo and D.A. Hastings, August 1993.

NESDIS 73 Intercomparison of the Operational Calibration of GOES-7 and METEOSAT-3/4. W. Paul Menzel, Johannes Schmetz, Steve Nieman, Leo Van de Berg, Volker Gaertner, and Timothy J. Schmit, September 1993.

NESDIS 74 Dobson Data Re-Evaluation Handbook. R. D. Hudson and W.G. Planet (Eds), October 1993.

NESDIS 75 Detection and Analysis of Fog at Night Using GOES Multispectral. Gary P. Ellrod, February 1994.

NESDIS 76 TOVS Operational Sounding Upgrades: 1990-1992. A. Reale, M. Chalfant, R. Wagoner, T. Gardner and L. Casey, March 1994.

NESDIS 77 NOAA Polar Satellite Calibration: A System Description. Cecil A. Paris, April 1994.

NESDIS 78 Post-Launch Calibration of the Visible and Near Infrared Channels of the Advanced Very High Resolution Radiometer on NOAA-7,-9, and -11 Spacecraft. C. R. Nagaraja Rao and Jianhua Chen, April 1994.

NESDIS 79 Quality Control and Processing of Historical Oceanographic Nutrient Data. Margarita E. Conkright, Timothy P. Boyer and Sydney Levitus, April 1994.

NESDIS 80 Catalogue of Heavy Rainfall Cases of Six Inches or More Over the Continental U.S. During 1993. Richard Borneman and Charles Kadin, August 1994.

NOAA Technical Report NESDIS 106

CALIBRATION OF THE ADVANCED MICROWAVE SOUNDING UNIT-A RADIOMETERS FOR NOAA-N AND NOAA-N'

Tsan Mo
NOAA/NESDIS/ORA/CRAD
5200 Auth Road, WWB/810
Camp Springs, MD 20746

Washington, DC
September 2002

U.S. DEPARTMENT OF COMMERCE
Donald L. Evans, Secretary

National Oceanic and Atmospheric Administration
Vice Admiral Conrad C. Lautenbacher, Jr., U.S. Navy (Ret.), Under Secretary

National Environmental Satellite, Data, and Information Service
Gregory W. Withee, Assistant Administrator

TABLE OF CONTENTS

TABLE CAPTIONS

FIGURE CAPTIONS

CALIBRATION OF THE ADVANCED MICROWAVE SOUNDING UNIT-A RADIOMETERS FOR NOAA-N AND NOAA-N'

Tsan Mo
NOAA/NESDIS
Office of Research and Applications
5200 Auth Road, Camp Springs, MD 20746

ABSTRACT

After successful launches of NOAA-K, -L, and -M, receptively, in 1998, 2000, and 2002, NOAA will launch its next two satellites, NOAA-N and -N' within next few years. Both will carry the Advanced Microwave Sounding Unit-A (AMSU-A) instruments. This report concerns the analysis and evaluation of the thermal-vacuum chamber calibration data from the two AMSU-A flight models for NOAA-N and -N'. These pre-launch calibration data were analyzed to evaluate the instrument performance, including calibration accuracy, nonlinearity, and temperature sensitivity. Great effort was taken to understand the instrument's radiometric performance as a function of instrument temperature. The calibration data provide a base for derivation of the calibration parameters input data sets (CPIDS) which will be incorporated into the NOAA operational calibration algorithm for producing the AMSU-A 1B data sets.

The nonlinearity parameters, which will be used for correcting the nonlinear contributions from an imperfect square-law detector, were determined from this data analysis. The existence and magnitude of nonlinearity in each channel were established and simulated with a quadratic formula for modeling the nonlinear contributions developed in the analysis of the NOAA-KLM AMSU-A pre-launch calibration data. The model was characterized by a single parameter u, values of which were obtained for each channel via least-squares fit to the data. Quadratic corrections which would be expected from the on-orbit data after the launch of AMSU-A into space were simulated. In these simulations, the cosmic background radiance corresponding to a cold space temperature 2.73K was adopted as one of the two reference points of calibration. The largest simulated nonlinear correction is about 2 K. Experience learned from examining the NOAA-15, -16, and -17 AMSU-A on-orbit data provides a better understanding of the AMSU-A performance in space and helps process these pre-launch calibration data. The calibration information presented in this report will be useful for post launch on-orbit verification of the AMSU-A instrument performance.

1. INTRODUCTION

On 13 May 1998, the NOAA-K, which is designated NOAA-15 after the launch, was successfully launched into a circular, near-polar orbit with an altitude of 833-km above the Earth and an inclination angle of 98.7° to the Equator. NOAA-15 carries the first of a series of new microwave total-power radiometers, the Advanced Microwave Sounding Units (AMSU-A and AMSU-B), which provide 20 channels for atmospheric temperature and moisture soundings. NOAA-L/16, which was launched on September 28, 2000, carries the second AMSU-A. The NOAA-M/17 AMSU-A was successfully launched on June 24, 2002. NOAA-17 is the first NOAA satellite that has been launched into an orbit to cross the Equator at 1000 and 2200 local time. NOAA-N and -N' will be launched in 2004 and 2008, respectively.

The AMSU-A is divided into two physically separate modules, each of which operates and interfaces with the spacecraft independently. The AMSU-A1 module uses two independent antenna-radiometer systems (A1-1 and A1-2) to provide 12 channels in the range of 50.3 to 57.3 GHz oxygen band for retrieving the atmospheric temperature profiles from the Earth's surface to about 50 kilometers (or 1 mb), and another channel at 89 GHz. The AMSU-A2, which has 2 channels at 23.8 and 31.4 GHz, are used to identify precipitation and correct the effect of surface emissivity, atmospheric liquid water, and water vapor on temperature sounding. These window channels are also used to derive rain rate, sea ice concentration, and snow cover.

Table 1 lists some of the NOAA-N AMSU-A main channel characteristics, including channel frequency, number of bands, 3-dB RF band width, radiometric temperature sensitivity (or NEΔT), antenna beam efficiency, polarization, and field of view (FOV) angular beam width for each channel. More detailed information on the AMSU-A radiometers is reported elsewhere [1]. Each of the AMSU-A antenna systems requires to have a nominal FOV of 3.3° at the half-power points and to cover a cross-track scan of ±48°20' (to beam centers) from the nadir direction with 30 Earth FOVs per scan line. Beam positions 1 and 30 are the outermost scan positions of the Earth views, while beam positions 15 and 16 (at ±1.67° from nadir) straddle the nadir. Views of cold space and a black-body target at the end of scan provide onboard calibration once each scan (8 sec).

The U. K. Meteorological Office provides the AMSU-B for humidity sounding. It has two channels at 89 and 150 GHz, respectively, and three channels around the 183 GHz water vapor line, detailed description of the AMSU-B radiometric performance has been given elsewhere [2].

Table 1. NOAA-N channel characteristics and specifications (AMSU-A1 S/N 109 and A2 S/N 105).

Channel	Channel Frequency (MHz)		No. of	Measured 3-dB RF Bandwidth	NEDT (K)		Beam #	Polarization	FOV**
Number	Specification	Measured *	Bands	(MHz)	Spec.	Measured	Efficiency	(NADIR)	(deg.)
1	23800	23800.20	1	251.00	0.30	0.208	96%	V	3.54
2	31400	31399.19	1	160.80	0.30	0.187	97%	V	3.41
3	50300	50300.54	1	160.20	0.40	0.246	96%	V	3.48
4	52800	52800.20	1	380.08	0.25	0.149	95%	V	3.42
5	53596 ± 115	53595.94 ± 115	2	167.48 | 167.48	0.25	0.169	96%	H	3.47
6	54400	54400.07	1	380.36	0.25	0.128	97%	H	3.41
7	54940	54940.21	1	380.18	0.25	0.148	97%	V	3.44
8	55500	55500.30	1	309.76	0.25	0.181	96%	H	3.45
9	fo = 57290.344	fo = 57290.342	1	310.08	0.25	0.166	97%	H	3.32
10	fo ± 217	fo ± 217	2	76.33 | 76.33	0.40	0.210		H	
11	fo ± 322.2 ± 48	fo ± 322.2 ± 48	4	34.86 / 35.37 | 35.37 / 34.86	0.40	0.243		H	
12	fo ± 322.2 ± 22	fo ± 322.2 ± 22	4	15.43 / 15.50 | 15.50 / 15.43	0.60	0.338		H	
13	fo ± 322.2 ± 10	fo ± 322.2 ± 10	4	7.85 / 7.86 | 7.86 / 7.85	0.80	0.481		H	
14	fo ± 322.2 ± 4.5	fo ± 322.2 ± 4.5	4	2.93 / 2.94 | 2.94 / 2.93	1.20	0.775		H	
15	89000	89008.00	1	1993.80	0.50	0.112	99%	V	3.26

* At temperature 22 degree C. ** Specification is required to have 3.3 degrees ± 10%. # Measured.

All of the AMSU-A flight models were tested and calibrated in a thermal-vacuum (TV) chamber by the contractor. These pre-launch TV calibration data were evaluated and analyzed to derive the calibration parameters input data set (CPIDS) which is used in the NOAA operational calibration algorithm to produce the AMSU-A 1B data sets. Particularly, there is a small nonlinearity (of the order of 1 K or less), which cannot be evaluated by the two-point calibration but is determined from the pre-launch calibration data.

In this study, the TV test data from the NOAA-N and -N' AMSU-A instruments are analyzed and evaluated. The same procedure developed for NOAA-K AMSU-A calibration [1] is closely followed. Experience gained from examining the NOAA-15 and NOAA-16 AMSU-A on-orbit data provides a better understanding of the AMSU-A performance in space and helps improve the analysis of the pre-launch calibration data. Some samples of AMSU-A on-orbit data are presented to demonstrate the dynamic variation of the calibration coefficients and calibration counts as a function of instrument temperature.

In the following sections, the results from the data analysis are presented. Instrument performances evaluated in this analysis include calibration accuracy, nonlinearity, and radiometric temperature sensitivity (or NEΔT, the noise-equivalent temperature). Section 1 gives an introduction and section 2 presents a brief description of the TV chamber test data. The calibration algorithm is described in section 3. The NOAA-N results are presented in section 4, while Appendix B has the NOAA-N' results. Conclusion and discussion are in section 5. Tables of CPIDS for NOAA-N and -N' are given in Appendices A and B, respectively. A brief description of the NOAA Level 1B data is given in Appendix C, which also contains some samples of AMSU-A on-orbit calibration coefficients and radiometric blackbody and space counts.

2. DESCRIPTION OF CALIBRATION DATA

Aerojet (now Northrop Grumman), the AMSU-A contractor, took the calibration data in a TV test chamber using the full scan mode. In this mode, AMSU-A scans through 30 Earth FOVs, the cold target, and the internal warm blackbody target once every 8 seconds. It takes one sample at each Earth FOV and two samples at the cold and warm targets, respectively. Since the scene calibration target was fixed at FOV 6 (31°40' from nadir), only radiometric counts from FOV 6 can be used for calibration. Each antenna system looks at its own individual cold, warm, and scene targets. A series of Platinum Resistance Thermometers (PRTs) were used to monitor the temperatures of these

Table 2. Number of PRTs in each calibration target and channels provided by individual antenna systems. The last row gives the number of scans collected in the calibration for each system.

Items	AMSU Antenna Systems			Remarks
	A2	A1-2	A1-1	
PRTs in Warm Target	7	5	5	
PRTs in Cold Target	11	7	7	
PRTs in Scene Target	11	7	7	
Channels	1 & 2	3, 4, 5 & 8	6, 7, & 9-15	
PLLO#2	-	-	Ch. 9-14	Backup PLLO
N(Scan No.)	120	400 to 900	400 to 900	See Note

Note: For A1-1 & A1-2: N=400, 400, 550, 725, 725, and 900 when the scene target temperature at T_s=84, 130, 180, 230, 280, and 330K, respectively.

---

calibration targets. The numbers of PRTs used to measure the physical temperatures of the scene, cold, and warm calibration targets in each antenna system are given in Table 2, which also lists the channels provided by each AMSU-A antenna system. Channels 9-14 have both primary and secondary phase locked loop oscillators (called PLLO #1 and PLLO #2, respectively) built-in. The PLLO #2 will be used for backup if PLLO #1 fails in operation. Invar high-Q cavity stabilized local oscillators [3] are used in other channels.

The physical temperatures of scene and cold targets measured by individual PRTs were provided in Kelvin (K) on Aerojet's data packages. However, the data from the PRTs monitoring the warm blackbody targets are given in counts, which are proportional to the blackbody temperatures. One should note that the scene and cold targets used in the TV chamber will not be carried into space. The PRT counts from the warm blackbody targets must be converted to PRT temperatures. The normal approach of deriving the PRT temperatures from counts is a two-step process: (1) the resistance of each PRT in ohms is computed by a count-to-resistance look-up table provided by the manufacturer. In this study, we used a polynomial representation of the count-to-resistance relationship provided by Aerojet; and (2) the individual PRT temperature in degrees Celsius is obtained from an analytic PRT equation [4], which is described in Appendix A. However, the two steps can be compressed to a single step with negligible errors. This single step process, which has been used in the NOAA-KLM calibrations, computes the PRT temperatures directly from the PRT counts, using a cubic polynomial

$$T_{Wk} = \sum_{j=0}^{3} f_{kj}\, C_k^j \tag{1}$$

where T_{Wk} and C_k represent the temperature and count of the PRT k. The polynomial coefficients, f_{kj}, are derived for each PRT in this study. Equation (1) also applies to 47 other housekeeping temperature sensors, such as the mixers, the IF amplifiers and the local oscillators. These f_{kj} coefficients for all PRTs and housekeeping sensors in NOAA-N AMSU-A1 S/N 109 and AMSU-A2 S/N 105 are listed in Appendix A (Tables A-1 and A-2, respectively), while the corresponding ones for the NOAA-N' AMSU-A are listed in Appendix B.

The mean internal blackbody temperature, T_W, is calculated from the individual PRT temperatures,

$$T_W = \frac{\sum_{k=1}^{m} W_k\, T_{Wk}}{\sum_{k=1}^{m} W_k} + \Delta T_W \tag{2}$$

where m represents the number of PRTs for each antenna system (as listed in Table 2) and W_k is a weight assigned to each PRT k. The quantity ΔT_W is a warm load correction factor, which is derived for each channel from the TV test data at three instrument temperatures (low, nominal, and high). The procedure for determining the ΔT_W values has been described elsewhere [5]. For each AMSU-A antenna system, a special set of calibration data was taken to determine the ΔT_W values, which are given in Appendix A (Table A-3). The W_k value, which equals 1 (0) if the PRT k is determined good (bad) before launch. Similarly, the mean temperatures of cold targets are defined in the same way as in Equation (2), except without the term ΔT_W.

The TV calibration data were taken at three instrument temperatures and the scene target was cycled through six temperatures 84, 130, 180, 230, 280, and 330K, respectively, at each instrument temperature. At each of the scene target temperatures, calibration data were acquired for enough number of scans to assure an effective temperature sensitivity less than 0.03K. The number of scans required depends upon the expected NEΔT of channel 14 (which has the largest NEΔT) and is therefore a function of the scene target temperature. Actual numbers of scans taken at individual temperatures are given in Table 2. The uncertainties in knowledge of brightness temperatures and measurement errors were obtained by Aerojet [6, 7]. These are given Table 3.

Table 3. Uncertainty in brightness temperatures and measurement errors.

Source of Error	AMSU-A2 :Ch. 1 and 2		AMSU-A1: Ch. 3 - 15	
	Bias (K)	Random (k)	Bias (K)	Random (k)
Warm Target	-0.050	±0.122	-0.050	±0.122
Cold Target	0.024	±0.105	0.024	±0.091
Scene Target	0.002	±0.101	0.002	±0.090

Antenna beam widths at all channels were also measured and the values for NOAA-N are listed in Table 1. Antenna beam efficiency at each channel frequency is greater than 95% and Table 1 lists the calculated values.

3. CALIBRATION ALGORITHM

In this study, calculations of radiometric measurements and variables related to the calibration process are all performed in radiance with dimension of mW/(m^2-sr-cm^{-1}), but the final results are presented in temperatures. All instruments flown on NOAA satellites produce measurements in radiance. Conversion between brightness temperature and radiance was performed using the full Planck function, instead of the Rayleigh-Jeans approximation. This also eliminates any possible conversion inaccuracy that may occur, particularly in the region of the space cosmic back-ground temperature ~2.73K, where the Rayleigh-Jeans approximation breaks down.

For each scan, the blackbody radiometric counts C_W are the averages of two samples of the internal blackbody. Similarly, the space radiometric counts C_C are the average of two samples of the space target. To reduce noise in the calibrations, the C_X (where X=W or C) for each scan line were convoluted over several neighboring scan lines according to a weight function [1]

$$\overline{C}_X = \frac{\sum_{i=-n}^{n} W_i C_X(t_i)}{\sum_{i=-n}^{n} W_i} \qquad \textbf{(3)}$$

where t_i (when $i \neq 0$) represents the time of the scan lines just before or after the current scan line and t_0 is the time of the current scan line. One can write $t_i = t_0 + i\Delta t$, where $\Delta t = 8$ seconds for AMSU-A. The 2n+1 values are equally distributed about the scan line to be calibrated. Following the NOAA-KLM operational preprocessor software, the value of n=3 is chosen for all AMSU-A antenna systems. A set of triangular weights of 1, 2, 3, 4, 3, 2 and 1 is chosen for the weight factor W_i that appears in Equation (3) for the seven scans with i = -3, -2, -1, 0, 1, 2, and 3.

The calibration algorithm [1], which takes into account the nonlinear contributions due to an imperfect square-law detector, converts scene counts to radiance R_S as follows,

$$R_S = R_W + \left(R_W - R_C\right)\left(\frac{C_S - \overline{C}_W}{\overline{C}_W - \overline{C}_C}\right) + Q \qquad \textbf{(4)}$$

where R_W and R_C are the radiance computed from the PRT blackbody temperature T_W and the PRT cold target temperature T_C, respectively, using the Planck function. The C_S is the radiometric count from the Earth scene target. The averaged blackbody and space counts, $\overline{C_W}$ and $\overline{C_C}$, are defined by Equation (3). The quantity Q, which represents the nonlinear contribution, is given by [1]

$$Q = u\left(R_W - R_C\right)^2 \frac{\left(C_S - \overline{C}_W\right)\left(C_S - \overline{C}_C\right)}{\left(\overline{C}_W - \overline{C}_C\right)^2} \qquad \textbf{(5)}$$

where u is a free parameter, values of which are determined at three instrument temperatures (low, nominal, and high). After launch of the instruments, the u values at the actual on-orbit instrument temperatures will be interpolated from these three values. For channels 9-14 (AMSU-A1-1), two sets of the u parameters are provided; one set is for the primary PLLO#1 and the other one for the redundant PLLO#2.

The quantity R_S in Equation (4) represents the radiometric scene radiance of individual channels. For users of NOAA Level 1B data, a simplified formula, which converts C_S directly into R_S, is presented in Appendix C. It should be noted that the ratios in Equations (4) and (5) will eliminate the effect of any linear variation in the radiometric counts on R_S. The channel gain, G, is defined as

$$G = \frac{\overline{C}_W - \overline{C}_C}{R_W - R_C} \tag{6}$$

The quantity G varies with instrument temperature, which is defined as the RF Shelf temperature for each AMSU-A antenna system. For a fixed instrument temperature, G is approximately constant. The first two terms in Equation (4) constitute a linear two-point calibration equation, if the quadratic term is negligible. Let R_{SL} denote these two terms,

$$R_{SL} = R_W + \left(R_W - R_C\right)\left(\frac{C_S - \overline{C}_W}{\overline{C}_W - \overline{C}_C}\right) \tag{7}$$

The linear scene radiance R_{SL} are calculated from the TV chamber test data. The results are given in the following section.

4. RESULTS

4.1 *Calibration Accuracy*

The calibration accuracy, ΔR, is defined as the difference between the scene PRT radiance R_{sprt} and the radiometric scene radiance. It is calculated from the equation

$$\Delta R = \frac{1}{N}\left[\sum_{i=1}^{N}\left(R_{sprt} - R_{SL}\right)_i\right] \tag{8}$$

where N is the number of scans at a specific scene temperatures (N= 120 for AMSU-A2 channels but ranging from 400 to 900 for AMSU-A1 channels).

Equation (7) would be a good representation of the microwave radiometric scene radiance for a perfect square-law detector. Any deviation of the quantity R_{SL} from the measured scene PRT radiance R_{sprt} indicates the presence of either nonlinearity in the radiometer system or some other potential source of contamination in the calibration data.

Figure 1 shows the calculated calibration accuracies in temperature, ΔT (corresponding to ΔR), versus the scene PRT temperature for channels 1 through 15. The AMSU-A specification requires $\Delta T = 2.0K$ for channels 1, 2, and 15, and $\Delta T = 1.5K$ for all other channels. The results in Figure 1 are better than the specification at all channels.

4.2 *Nonlinearity*

The ΔT patterns (Figure 1) show clearly the nonlinearity patterns which can be represented by the quadratic formula Q defined in Equation (5). The nonlinearity of a channel is normally defined as the residuals from a least-squares fit of its scene PRT radiance as a linear function of the radiometric radiance R_{SL} (Equation 7). The nonlinearity is defined as the differences (or residuals) between the R_{sprt} and the best-fit results from a linear equation in the form LinFit = a + bR_{SL} (where a and b are the intercept and slope). These residuals, which are defined as the measured nonlinearity Q (= R_{sprt} - LinFit), are shown in Figure 2. The largest (absolute) Q value on each curve is defined as measured nonlinearity that can be compared to those as defined in the AMSU-A specification.

The results in Figure 2 show that the maximum (absolute) Q values are about 0.7K. The AMSU-A specification requires Q = 0.5K for channels 1, 2, and 15; and Q = 0.375K for other channels. Some results in Figure 2 do not meet the specifications. Most of the curves in Figure 2 have two roots, representing solutions of a quadratic equation, which can be written in the form

$$Q = u\left(R_S - R_1\right)\left(R_S - R_2\right) \tag{9}$$

where R_1 and R_2 represent the two roots. One can obtain a similar equation from Equation (5) by replacing the counts by its individual radiance, since the radiometric counts are proportional to radiance in a first-order approximation. The resultant equation represents a different straight line intersecting the same curve at R_W and R_C. Once the parameter u is determined, it can be used with any pair of roots to calculate Q. We applied Equation (9) to fit the quadratic curves in Figure 2 to obtain the u values with the two roots extracted from each plot. Table 4 gives the best-fit u values at three instrument temperatures for individual channels.

NOAA-N: AMSU-A2 S/N 105 RF-Shelf Temperature (C): xx= -6.2, **=12.2, ++=30.7
AMSU-A1 S/N 109 RF-Shelf Temperature (C): xx= -2.3, **=18.2, ++=38.0

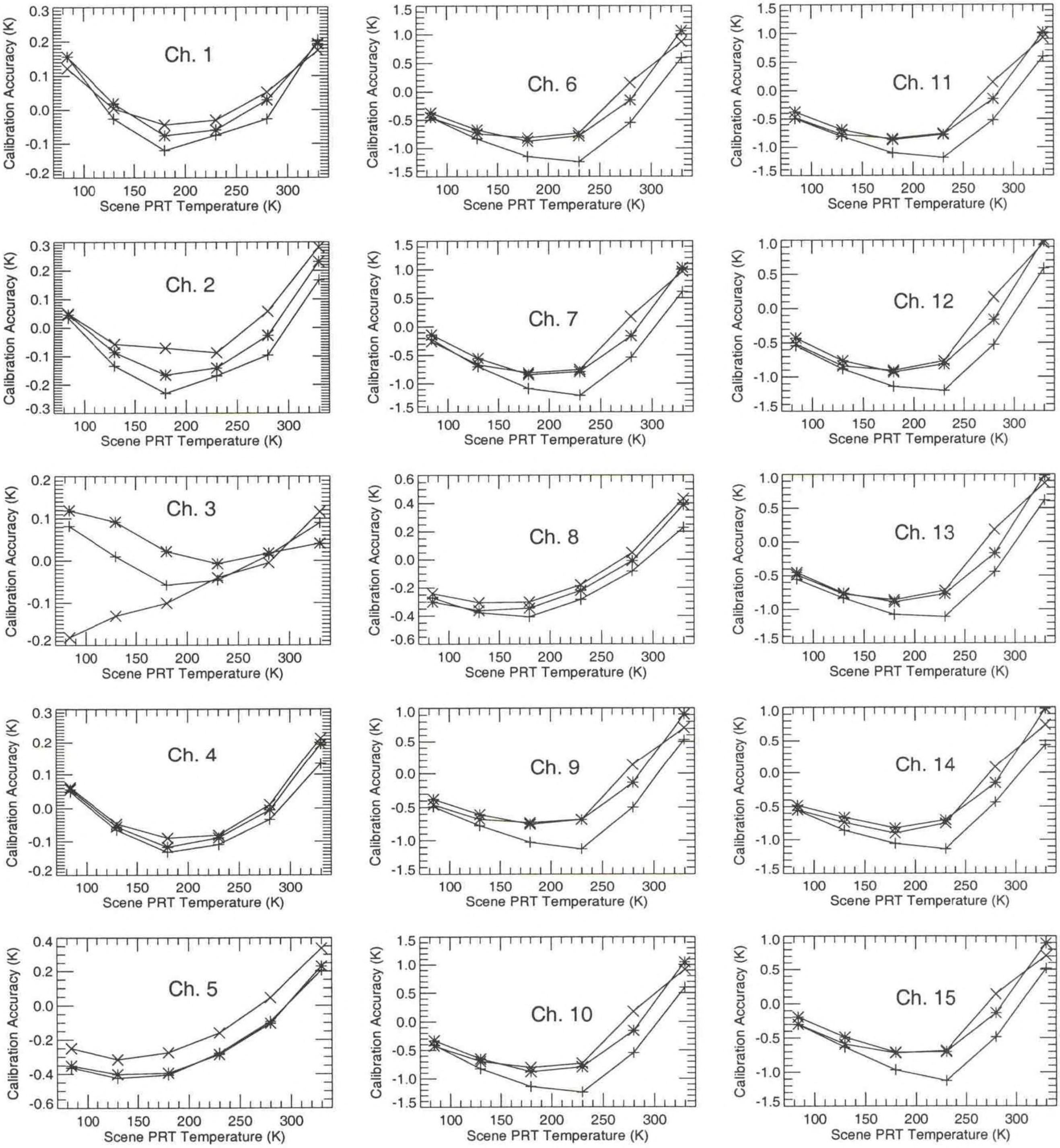

Figure 1. NOAA-N AMSU-A: Calibration accuracies at three instrument temperatures.

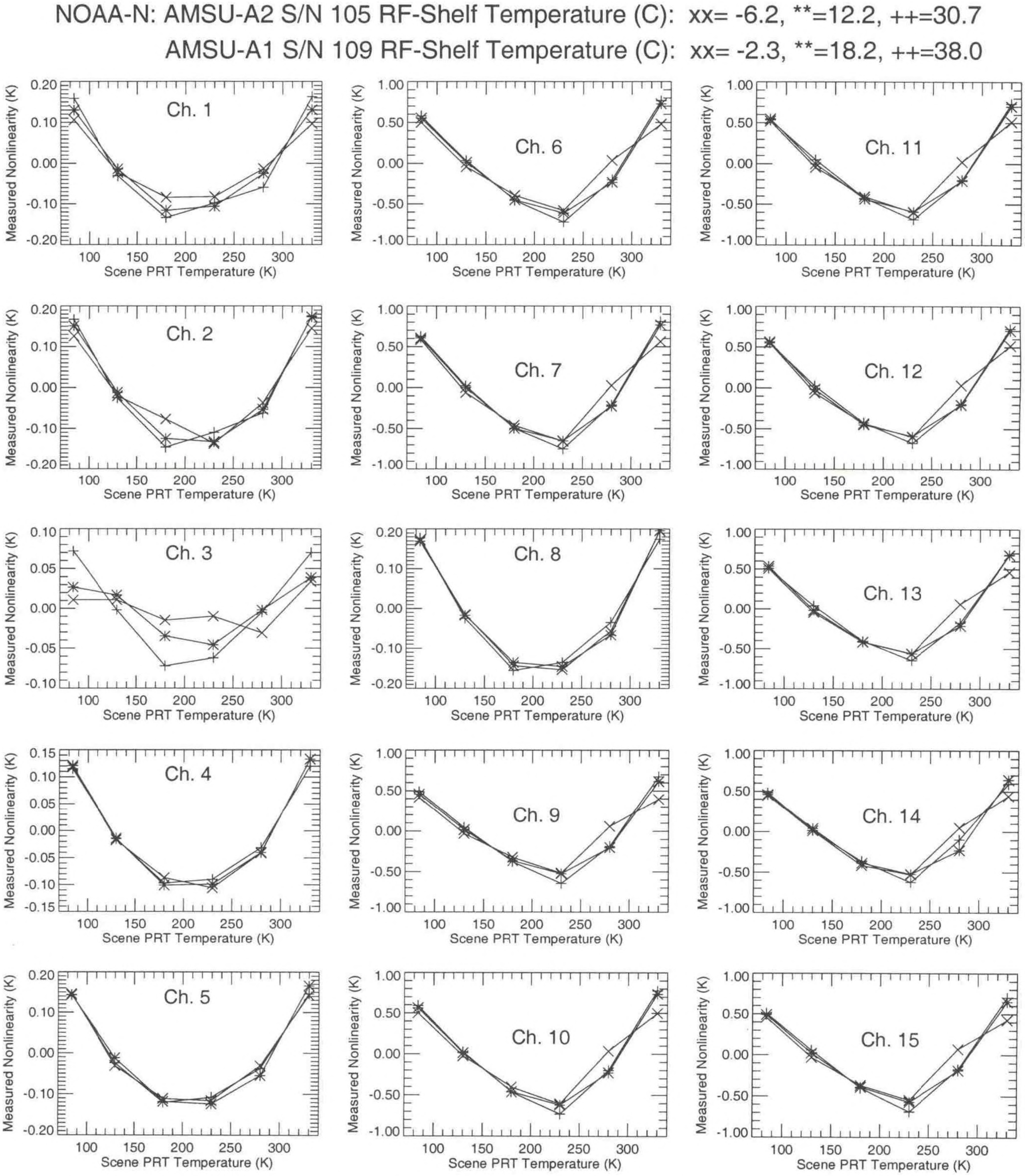

Figure 2. NOAA-N AMSU-A: Residuals after least-squares fit of the scene PRT radiance as a function of R_{SL} as discussed in the text.

Table 4. NOAA-N nonlinearity parameters u in dimension of (m^2-sr-cm^{-1})/mW.

AMSU-A2 S/N 105 channels: **AMSU-A1-2 S/N 109 channels:**

Instrument Temp.(C)	Ch.1	Ch.2	Instrument Temp.(C)	Ch.3	Ch.4	Ch.5	Ch.8
-6.24	2.408068	1.858443	-2.35	0.080118	0.601668	0.675368	0.808420
12.18	3.156231	2.207761	18.30	0.166955	0.612502	0.720600	0.791947
30.66	3.724993	2.302441	38.26	0.384415	0.566881	0.680903	0.776335

AMSU-A1-1 S/N 109 channels: PLLO#1

Instrument Temp.(C)	Ch.6	Ch.7	Ch.9	Ch.10	Ch.11	Ch.12	Ch.13	Ch.14	Ch.15
-2.33	2.250542	2.591933	1.661441	2.079052	2.147850	2.198723	1.977414	1.832619	0.746548
18.26	2.891682	3.074492	2.174950	2.643677	2.563977	2.613077	2.491425	2.181756	0.958614
38.18	3.041596	3.201168	2.330455	2.797101	2.544715	2.601223	2.411822	2.248804	1.002658

AMSU-A1-1 S/N 109 channels: PLLO#2

Instrument Temp.(C)	Ch.9	Ch.10	Ch.11	Ch.12	Ch.13	Ch.14
-2.41	2.111449	2.540336	2.616352	2.693440	2.517332	0.922610
18.19	2.043021	2.600622	2.457046	2.498281	2.281584	0.839327
38.17	2.120067	2.625359	2.388372	2.512140	2.295614	0.876285

4.3 Simulated Quadratic Corrections to On-Orbit Data

Once the u values are determined, Equation (9) can be used to simulate the quadratic contributions which are expected from on-orbit data. This can be accomplished by replacing the roots R_1 and R_2 with the radiance $R_{2.73}$ (corresponding to cold space temperature 2.73K) and R_W, respectively. The simulated results are shown in Figure 3 for all channels at three instrument temperatures which are listed at the top of the plots. One should note that the instrument temperatures are different for the AMSU-A antenna systems. The simulated quadratic contributions displayed in Figure 3 are larger than those shown in Figure 2. This is expected because the separation of the two reference calibration points is increased in the cases of simulations. Noticeable quadratic contributions appear in all channels, particularly the AMSU-A1-1 channels. The largest ones are approximately 2 K at several channels. It is important to note that the effect of instrument temperature on the quadratic contributions is nonlinear in general.

Similarly, Figure 4 shows the calculated results which are associated with the redundant PLLO#2 built into channels 9-14. The left column of Figure 4 displays the calibration accuracies, ΔT, which are similar to Figure 1 and the middle column (corresponding to Figure 2) shows the residuals of the least-squares fit. The right column shows the simulated quadratic corrections, Q, which would occur in on-orbit data.

4.4 Temperature Sensitivity

The temperature sensitivity (or NEΔT) specification for AMSU-A channels are listed in Table 1. It is defined as the minimum change of a scene brightness temperature that can be detected. In practice, it is calculated as the standard deviation of the radiometer output (in K), when an antenna system is viewing a scene target at 300K. The calculated NEΔT values are shown in Figure 5 together with the AMSU-A specifications. These calculated NEΔT values correspond to a scene temperature of 305K, because they are the average values of two measurements taken at the scene target temperatures of 280K and 330K, respectively (no calibration data were taken at 300K). All of the calculated NEΔT values in Figure 5 are better than those given in the AMSU-A specification. Actually, all NEΔT values measured at both 280 and 330K are better than the specification. The calculated NEΔT values at other instrument temperatures are shown in Figure 6. In general, the NEΔT value decreases as the instrument temperature becomes colder.

NOAA-N: AMSU-A2 S/N 105 RF-Shelf Temperature (C): xx= -6.2, **=12.2, ++=30.7
AMSU-A1 S/N 109 RF-Shelf Temperature (C): xx= -2.3, **=18.2, ++=38.0

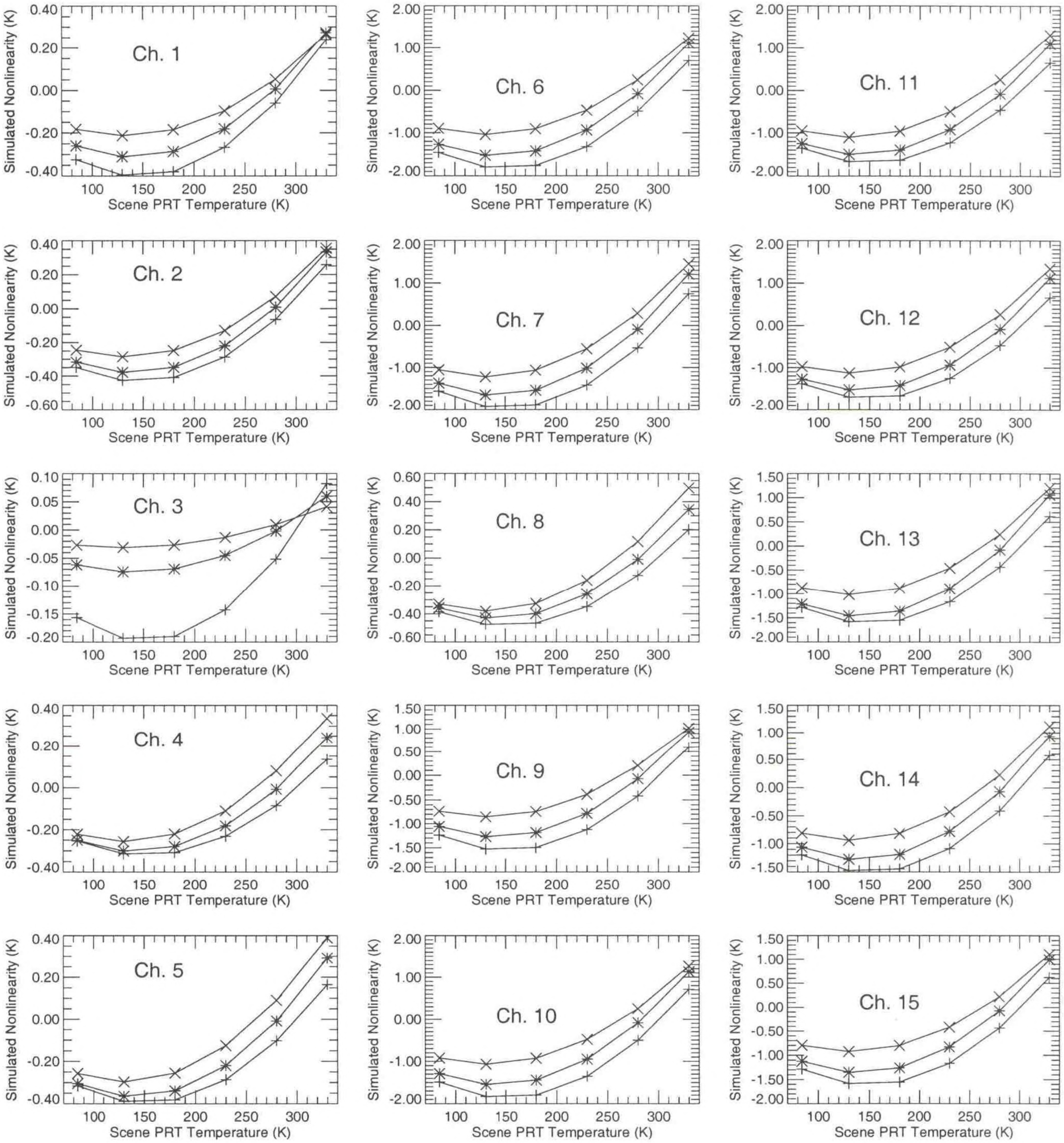

Figure 3. NOAA-N AMSU-A: Simulated nonlinearity as expected from on-orbit data.

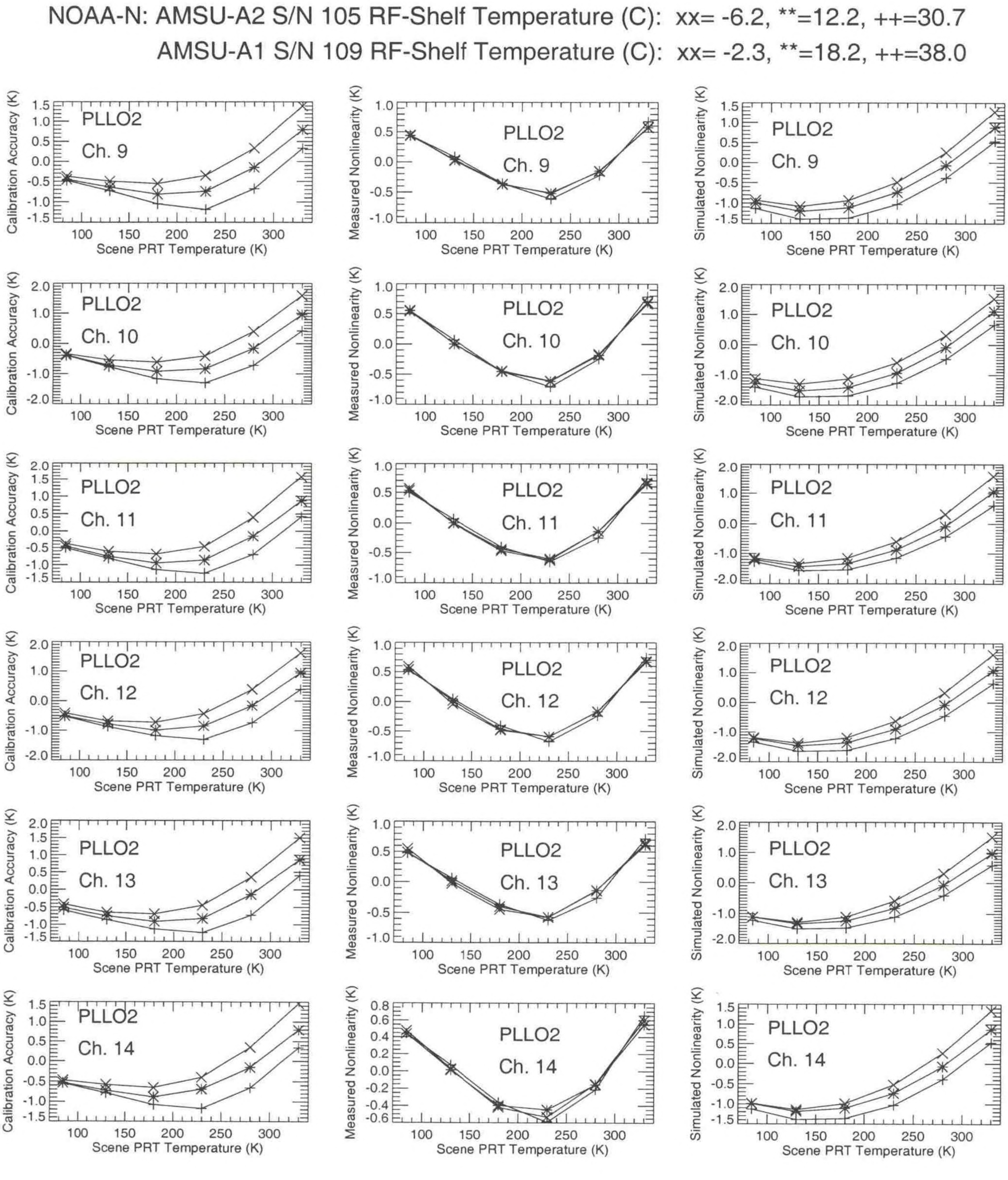

Figure 4. NOAA-N AMSU-A: Calibration results withe PLLO #2 in Channels 9-14, including calibration accuracy, measured nonlinearity, and simulated nonlinearity.

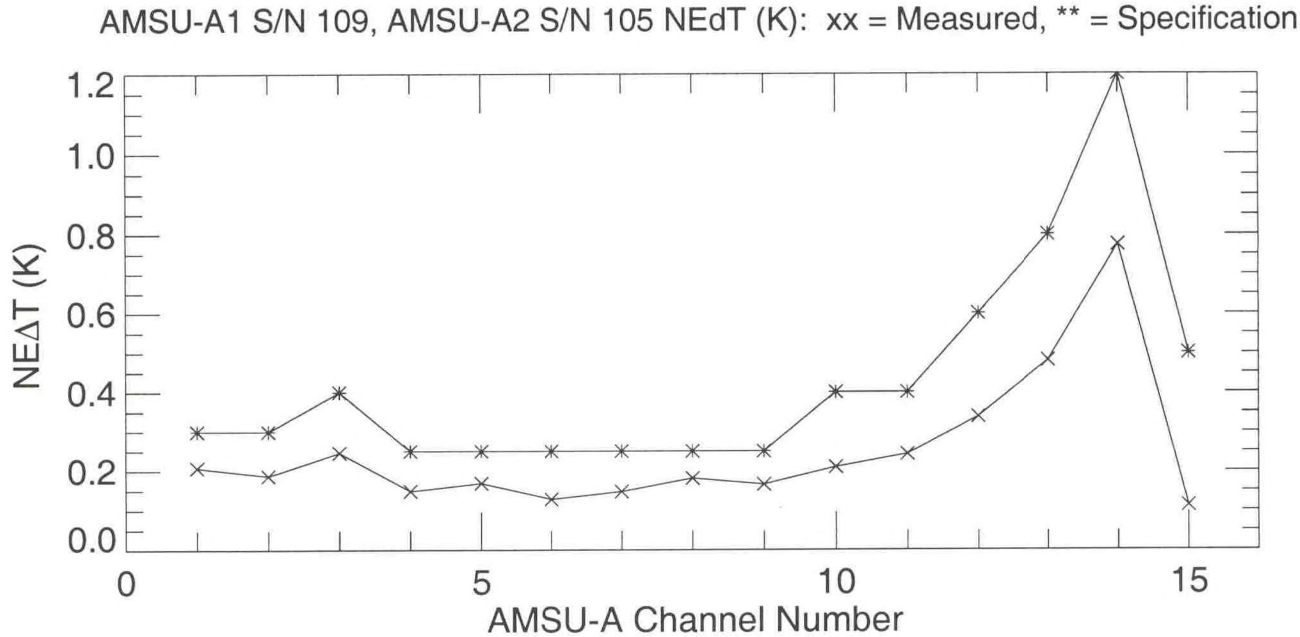

Figure 5. NOAA-N AMSU-A: Comparison of the measured NEΔT values with specification.

NOAA-N: AMSU-A2 S/N 105 RF-Shelf Temperature (C): xx= -6.2, **=12.2, ++=30.7
AMSU-A1 S/N 109 RF-Shelf Temperature (C): xx= -2.3, **=18.2, ++=38.0

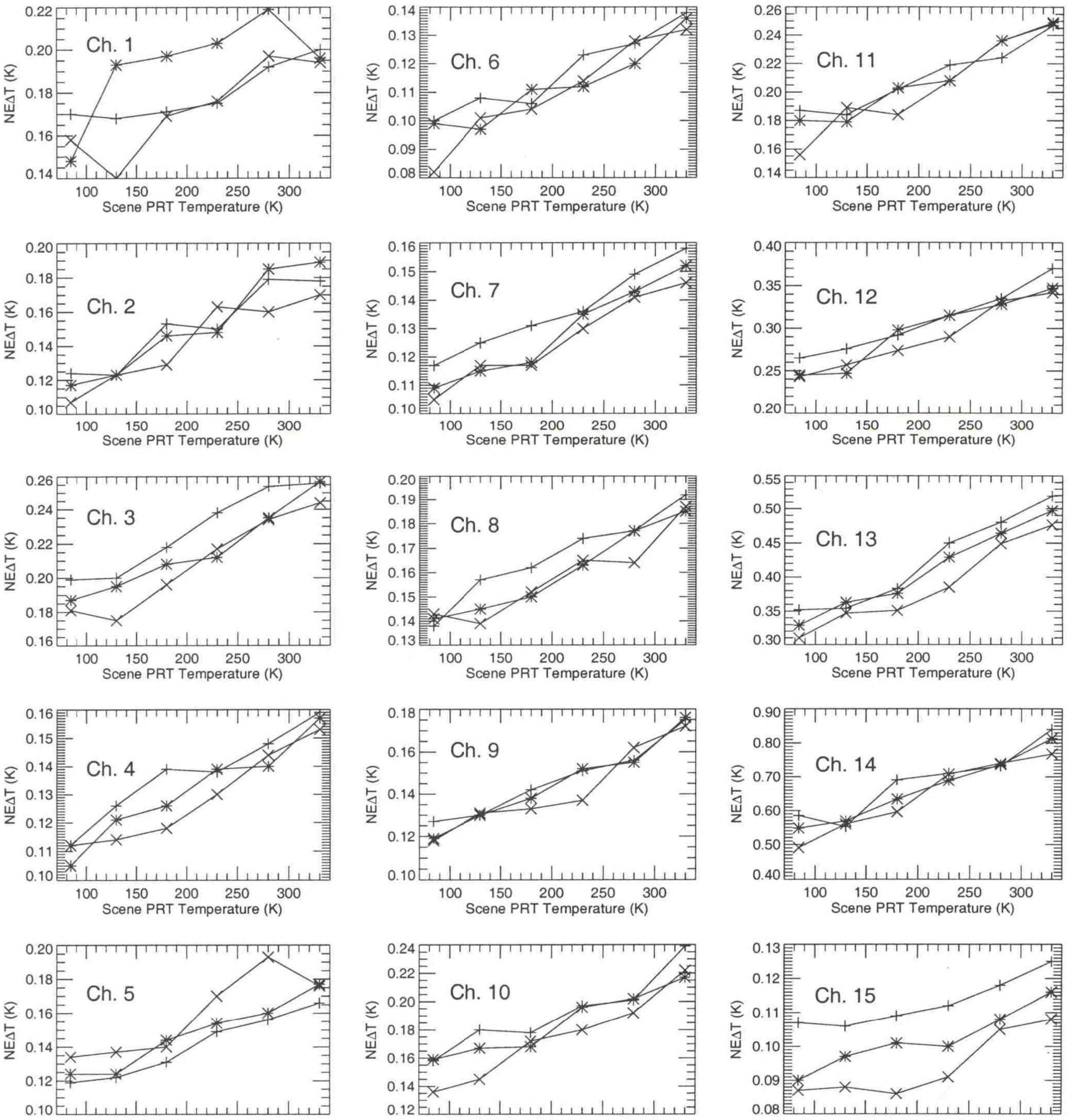

Figure 6. NOAA-N AMSU-A: Measured NEΔT values at three instrument temperatures.

4.5 Radiometric Counts at Zero Radiance

Figure 7 shows the plots of TV scene radiometric counts versus the scene PRT temperatures for all channels. The radiometric counts increase linearly with scene PRT temperatures ranging from 84 to 330K and good linear relationships exist between the radiometric counts and the scene PRT temperatures in the range 84 to 330K. One can extrapolate these linear relationships to 0 K (corresponding to zero radiance) and obtain the intercepts for these plots. The intercept for each data point can also be computed from Equation (7) by setting $R_{SL}= 0$ and solve for C_S, which is denoted by C_{Sint} as

$$C_{S\,\mathrm{int}} = \overline{C}_W - G\,R_W \qquad \textbf{(10)}$$

where G is the channel gain defined in Equation (6). The calculated C_{Sint} values at three instrument temperatures for each channel are shown in Figure 8. These are the mean values of all calculations performed with all available calibration data (from 120 to 900 scans as the scene temperature varies from 84 to 330K). At each instrument temperature, the variation in the calculated C_{Sint} values is relatively small and all C_{Sint} values are positive. Figure 8 shows that the instrument temperature has a big impact on the magnitude of C_{Sint}, which increases as the instrument temperature decreases.

4.6 Channel gains

Values of the channel gains as defined in Equation (6) are also calculated from the TV calibration data. The gain values are converted into dimension of count/K. Figure 9 shows the calculated channel gains at three instrument temperatures, which are listed at the top of Figure 9. One should note that the gains of Channel 15 are smaller than those of other channels by about a factor 2 and that the abnormal behavior of channel 1 gain as a function of instrument temperature. Similarly, Figure 10 shows the calculated results of channel gain, radiometric counts, and intercept counts as a function of the scene PRT temperature when PLLO#2 was used.

5. CONCLUSION AND DISCUSSION

The TV chamber calibration data for the NOAA-N AMSU-A, including A1 S/N 109 and A2 S/N 105, and the NOAA-N' AMSU-A, A1 S/N 105 and A2 S/N 107, were analyzed to derive the CPIDS which will be used in the NOAA operational calibration algorithm to produce the AMSU-A 1B data

NOAA-N: AMSU-A2 S/N 105 RF-Shelf Temperature (C): xx= -6.2, **=12.2, ++=30.7

AMSU-A1 S/N 109 RF-Shelf Temperature (C): xx= -2.3, **=18.2, ++=38.0

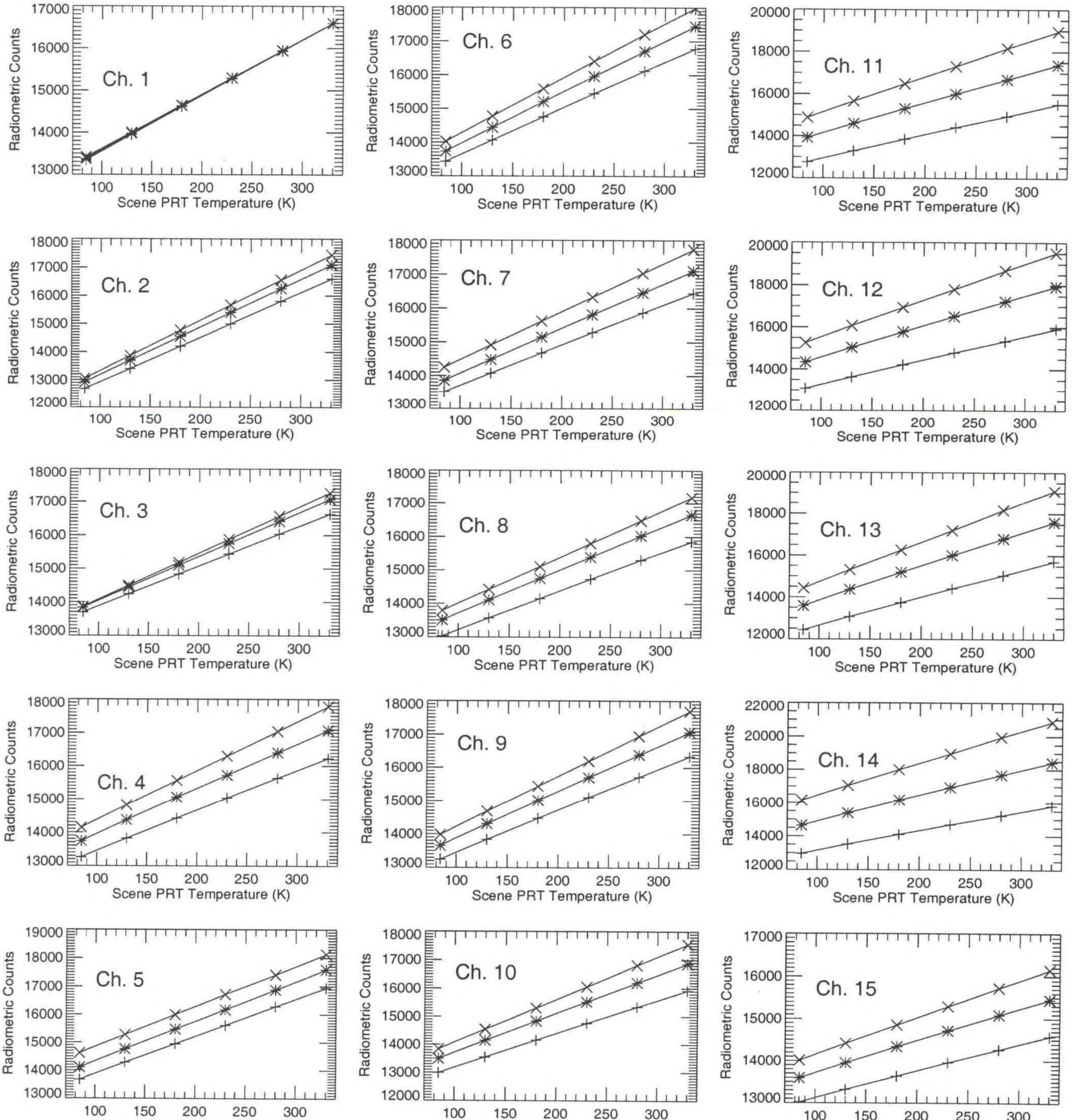

Figure 7. NOAA-N AMSU-A: Radiometric counts versus scene PRT temperature at three instrument temperatures

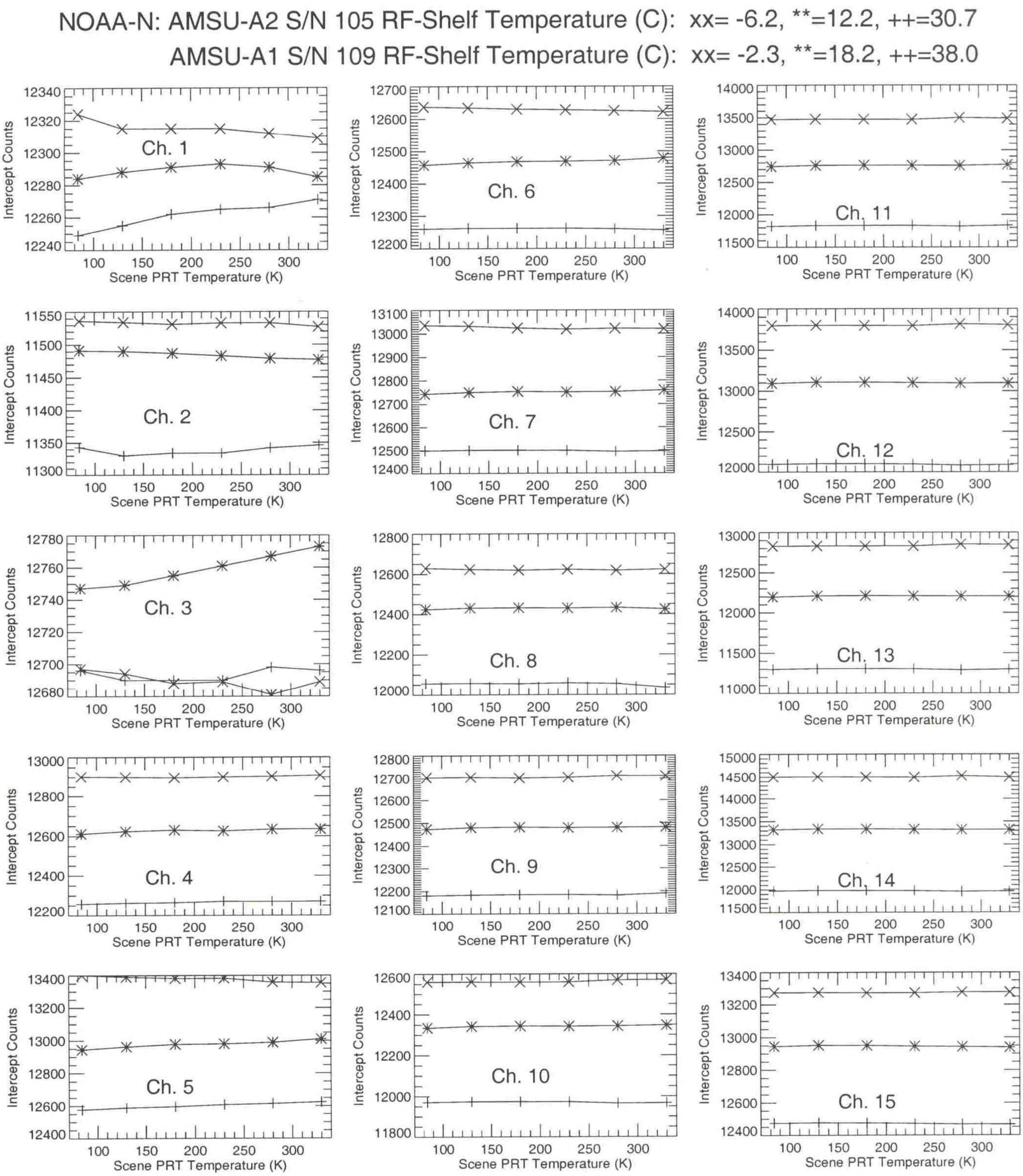

Figure 8. NOAA-N AMSU-A: Intercept counts at three instrument temperatures.

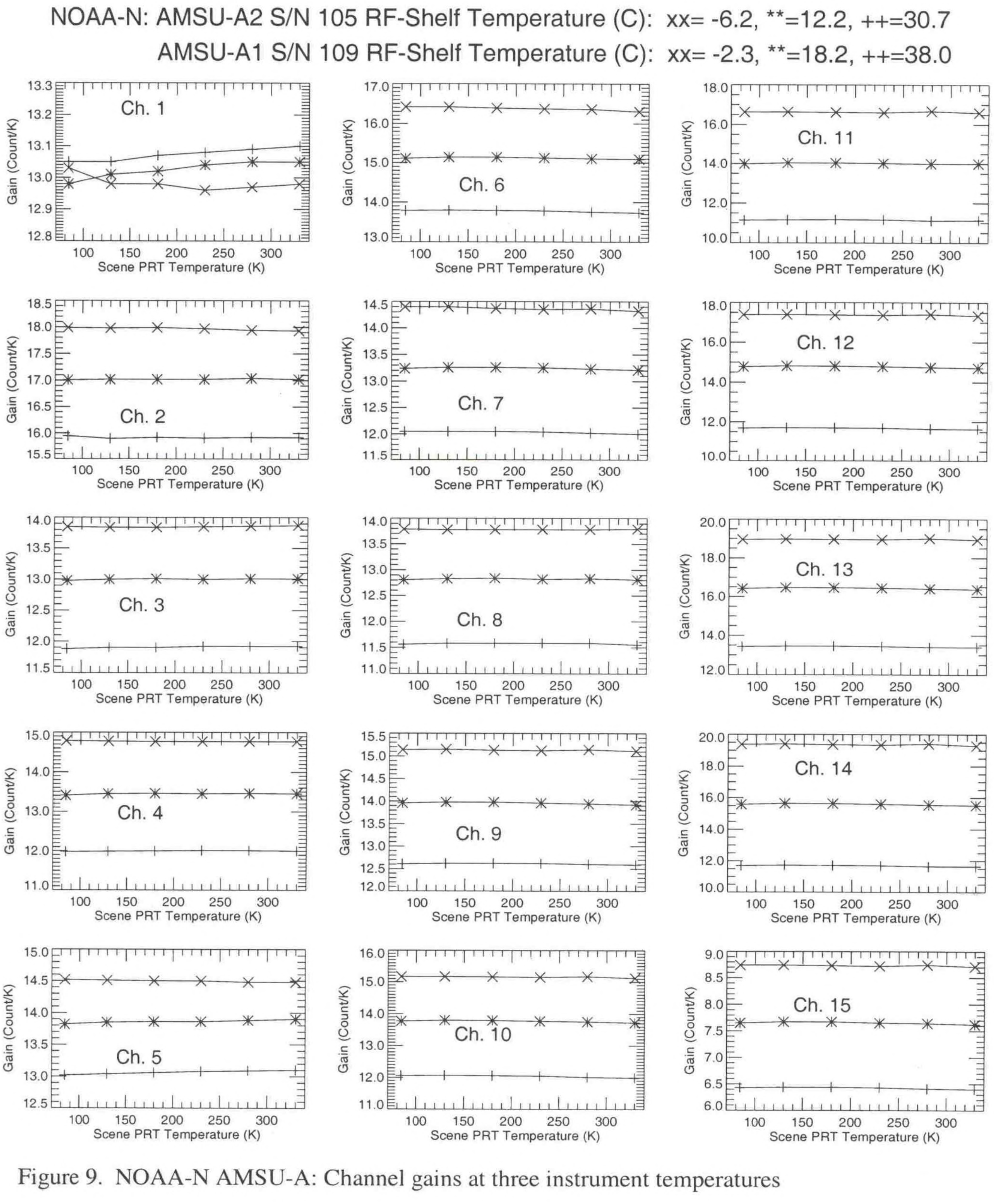

Figure 9. NOAA-N AMSU-A: Channel gains at three instrument temperatures

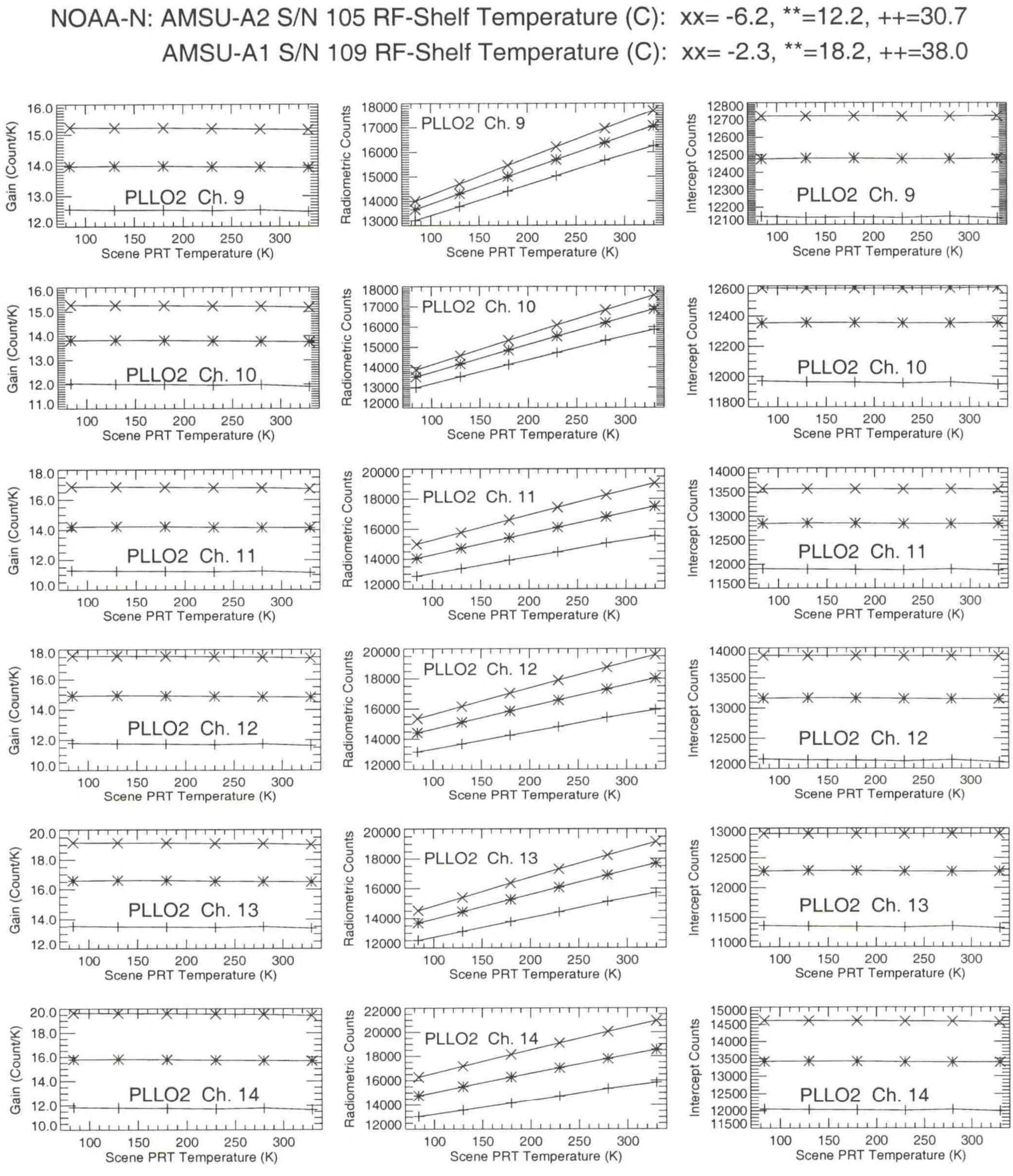

Figure 10. NOAA-N AMSU-A: Calibration results with PLLO #2 in Channels 9-14, including gains, radiometric counts, and intercept counts at three instrument temperatures.

sets. The results show that both sets of instruments meet the AMSU-A specification in calibration accuracy and temperature sensitivity, but the measured nonlinearities at several channels do not meet the AMSU-A specification.

The nonlinearity exists at all channels. A quadratic formula with a single parameter u is used to simulate these nonlinear contributions. The u values at three instrument temperatures were obtained from the pre-launch calibration data. Using the best-fit u values, the quadratic corrections which would be expected from the on-orbit data were simulated. In the simulations, the cold space radiance corresponding to 2.73K was adopted as one of the two reference calibration points (the other one is the internal blackbody temperature). The largest simulated nonlinear correction is about 2 K as shown in Figure 3.

Experience gained from examining the NOAA-15 and NOAA-16 AMSU-A on-orbit data provides a better understanding of the AMSU-A performance in space and helps process the pre-launch calibration data. Some samples of on-orbit AMSU-A data are presented in Appendix C to demonstrate the dynamic variations of the calibration coefficients and calibration counts as a function of scan number over an orbit. The time series of the calibration coefficients shows why they must be calculated at each scan lines and that the pre-launch values, which do not have the dynamic variation induced by the on-orbit changes in instrument temperature, can not be employed to convert the radiometric counts into temperatures.

In general, the qualities of the calibration data are quite good. Particularly, the instrument temperatures were stabilized at pre-selected values with total variation less than ±0.5K during each test cycle. This renders the measured instrument nonlinearities more reliable. The results presented in this study confirm the good quality of the AMSU-A instruments for both NOAA-N and -N'. The calibration information presented in this report will be immensely useful for post launch on-orbit verification of the AMSU-A instrument performance.

ACKNOWLEDGMENTS: The author would like to thank J. Philip Green of NOAA Liaison Office and Sergey Krimchansky of NASA/GSFC for their management of the AMSU-A Program. Aerojet, now Northrop Grumman, was the primary AMSU-A contractor for building the instruments and performed the initial calibration analysis to demonstrate the high quality of the instrument performance.

REFERENCES

[1]. Tsan Mo, "Prelaunch Calibration of the Advanced Microwave Sounding Unit-A for NOAA-K," IEEE Trans. Microwave Theory and Techniques, vol. 44, pp. 1460-1469, 1996.

[2]. R. W. Rogers, T. J. Hewison, N. C. Atkinson, and S. J. Stringer, "The radiometric Characterization of AMSU-B," IEEE Trans. Microwave Theory and Techniques, vol. 43, pp. 760-771, 1995..

[3]. P. K. Patel and J. Mentall, "The Advanced Microwave Sounding Unit-A," in *Microwave Instrumentation for Remote Sensing of the Earth,* SPIE Vol. 135, Orlando, April 13-14, 1993. pp.130-135.

[4]. PRT Handbook, Bulletin 1024, 1986, Rosemount Inc., Burnsville, MN 55337.

[5]. Tsan Mo, "Calibration of the Advanced Microwave Sounding Unit-A for NOAA-K," NOAA Technical Report NESDIS 85, June 1995.

[6]. "Calibration Log Book for AMSU-A2 S/N 105," Report No. 11323, May 1999, Aerojet, Azusa, CA 91702.

[7]. "Calibration Log Book for AMSU-A1 S/N 109," Report No. 11330, August 2000, Aerojet, Azusa, CA 91702.

[8]. "Calibration Log Book for AMSU-A2 S/N 107," Report No. 11322, June 1999, Aerojet, Azusa, CA 91702.

[9]. "Calibration Log Book for AMSU-A1 S/N 105," Report No. 11330, August 2000, Aerojet, Azusa, CA 91702.

[10]. Tsan Mo, "AMSU-A Antenna Pattern Corrections," IEEE Trans. Geoscience and Remote Sensing, vol. 37, pp. 103-112, 1999.

APPENDIX A

NOAA-N CPIDS : COEFFICIENTS OF AMSU-A1 S/N 109 AND AMSU-A2 S/N 105

A.1 *Polynomial Coefficients for Converting PRT Counts into Temperatures*

The two-step process for deriving the PRT temperatures from PRT counts C_k is briefly described here. First the count C_k from PRT k is converted into resistance r_k (in ohms) by a polynomial

$$r_k = \sum_{i=0}^{3} A_i \, C_k^i \tag{A-1}$$

where the coefficients A_i for individual PRTs and temperature sensors were provided by Aerojet. Once the resistance r_k is known, then one can calculate the PRT temperature t (in Celsius) from the Callendar-Van Dusen equation [6], which is given by

$$\frac{r_t}{r_o} = 1 + \alpha\left[t - \delta\left(\frac{t}{100} - 1\right)\frac{t}{100} - \beta\left(\frac{t}{100} - 1\right)\left(\frac{t}{100}\right)^3\right] \tag{A-2}$$

where: r_t = resistance (in ohms) at temperature t (°C) of the blackbody target

r_o = resistance at t = 0°C (supplied by the manufacturer via Aerojet)

β = 0 for t > 0°C, and 0.11 for t < 0°

α and δ are constants provided by the manufacturer via Aerojet.

Calculation shows that the error is negligible by setting $\beta = 0$ in Equation (A-2). In this study, it is assumed $\beta = 0$ in all cases, then Equation (A-2) is simplified into a quadratic equation in t. In such case, one can solve the quadratic equation for t in terms of r_t. Then the PRT temperature in degree Kelvin is obtained from t + 273.15. By this way, data sets of PRT temperatures versus counts for individual PRTs are computed. Then Equation (1) is applied to fit these data sets for obtaining the polynomial coefficients f_{kj} for individual PRTs and housekeeping sensors. These best-fit coefficients are listed in Tables A-1 and A-2, respectively, for AMSU-A1 S/N 109 and AMSU-A2 S/N 105. Test calculations show that these polynomials are highly accurate in reproducing temperatures of PRTs and sensors with errors in order of 0.01 K.

Table A-1. NOAA-N AMSU-A1 S/N 109: Polynomial coefficients for converting PRT counts into temperatures.

PRT No.	Description	Fk0 (K)	Fk1 (K/count)	Fk2 (K/count^2)	Fk3 (K/count^3)
1	Al-1 MOTOR	264.1476	1.743266E-03	3.348404E-09	1.664095E-14
2	Al-2 MOTOR	263.1678	1.731684E-03	3.541911E-09	1.427281E-14
3	Al-1 FEED HORN	263.4037	1.756592E-03	3.025439E-09	2.592502E-14
4	Al-2 FEED HORN	263.7585	1.736896E-03	3.524135E-09	9.021489E-15
5	Al-1 RF MUX	263.2661	1.734418E-03	3.627309E-09	1.270486E-14
6	Al-2 RF MUX	263.6731	1.710861E-03	3.745664E-09	1.954603E-14
7	CH. 3 DRO	263.2463	1.736519E-03	3.450645E-09	1.511849E-14
8	CH. 4 DRO	263.0471	1.729353E-03	3.629986E-09	1.108148E-14
9	CH. 5 DRO	263.4903	1.732073E-03	3.660650E-09	1.059084E-14
10	CH. 6 DRO	263.4986	1.743907E-03	3.378800E-09	1.731537E-14
11	CH. 7 DRO	263.4426	1.739730E-03	3.231359E-09	1.741037E-14
12	CH. 8 DRO	263.1023	1.739080E-03	3.435317E-09	1.558292E-14
13	CH. 15 GDO	262.9301	1.733167E-03	3.619563E-09	1.102405E-14
14	CH. 9 thru 14 PLO #2	262.2288	1.782365E-03	3.927203E-09	1.074884E-14
15	CH. 9 thru 14 PLO #1	263.3337	1.730256E-03	3.892761E-09	6.229168E-15
16	Not Used	263.3337	1.730256E-03	3.892761E-09	6.229168E-15
17	CH. 3 MIXER/IF	262.5283	1.728151E-03	3.730241E-09	1.055708E-14
18	CH. 4 MINER/IF	262.6262	1.735880E-03	3.482120E-09	1.463006E-14
19	CH. 5 MINER/IF	263.0344	1.729980E-03	3.817571E-09	1.028369E-14
20	CH. 6 MIXER/IF	263.3519	1.737770E-03	3.370750E-09	1.684445E-14
21	CH. 7 MIXER/117	263.5179	1.740044E-03	3.604026E-09	8.980608E-15
22	CH. 8 MIXER/IF	262.9976	1.731195E-03	3.710931E-09	1.056478E-14
23	CH. 9 thru 14 MIXER/IF	262.8521	1.733479E-03	3.670787E-09	1.256491E-14
24	CH. 15 MIXER/IF	263.6473	1.747099E-03	3.570097E-09	5.402493E-15
25	CH. 11 thru 14 IF AMP	263.3202	1.739659E-03	3.556506E-09	1.392298E-14
26	CH. 9 IF AMP	263.3429	1.735609E-03	3.941727E-09	8.254678E-15
27	CH. 10 IF AMP	263.0992	1.736573E-03	3.728037E-09	1.006676E-14
28	CH. 11 IF AMP	263.4255	1.735551E-03	3.770763E-09	5.931839E-15
29	DC/DC CONVERTER	263.7365	1.730352E-03	4.034858E-09	5.881655E-15
30	CH. 13 IF AMP	263.3358	1.738157E-03	3.671254E-09	1.245797E-14
31	CH. 14 IF AMP	263.1836	1.740586E-03	3.337613E-09	1.651644E-14
32	CH. 12 IF AMP	263.4875	1.735195E-03	3.754301E-09	1.074719E-14
33	Al-1 RFSHELF	264.1607	1.745635E-03	3.690702E-09	1.142299E-14
34	A1-2 RF SHELF	263.4113	1.743746E-03	3.503678E-09	1.460422E-14
35	DETECTOR/PRE-AMP	263.7069	1.735678E-03	3.727127E-09	1.026177E-14
36	Al-1 WARM LOAD 1	254.4792	1.632697E-03	5.925882E-09	2.790891E-14
37	Al-1 WARM LOAD 2	254.9357	1.632574E-03	5.837758E-09	2.895840E-14
38	Al-1 WARM LOAD 3	254.6461	1.628482E-03	5.867548E-09	2.882307E-14
39	Al-1 WARM LOAD 4	254.7101	1.628115E-03	5.919407E-09	2.831376E-14
40	A1-1 WARM LD CENTER	254.6003	1.605916E-03	8.652163E-09	-4.137281E-14
41	A1-2 WARM LOAD 1	255.4882	1.617997E-03	4.542892E-09	6.722034E-14
42	A1-2 WARM LOAD 2	254.5689	1.632253E-03	5.841521E-09	2.896778E-14
43	A1-2 WARM LOAD 3	254.4614	1.630541E-03	5.753884E-09	2.950770E-14
44	Al-2 WARM LOAD 4	254.7519	1.634664E-03	5.835678E-09	2.836517E-14
45	A1-2 WARM LD CENTER	254.8793	1.635115E-03	5.835015E-09	2.919876E-14

Table A-2. NOAA-N AMSU-A2 S/N 105: Polynomial coefficients for converting PRT counts into temperatures.

PRT No.	Description	Fk0 (K)	Fk1 (K/count)	Fk2 (K/count^2)	Fk3 (K/count^3)
1	Scan Motor	263.5758	1.767645E-03	3.794875E-09	1.261675E-14
2	Feedhorn	263.1411	1.764382E-03	3.661103E-09	1.305692E-14
3	RF Diplexer	263.1864	1.752475E-03	3.844197E-09	1.227221E-14
4	Mixer/IF CH1	263.8281	1.754974E-03	3.802008E-09	1.077093E-14
5	Mixer/IF CH2	263.7458	1.756229E-03	3.727035E-09	1.308870E-14
6	CH I DRO	263.9707	1.758280E-03	3.718871E-09	1.248273E-14
7	CH 2 DRO	263.4596	1.756287E-03	3.826887E-09	1.288159E-14
8	Compensat Motor	263.9833	1.757519E-03	3.769221E-09	1.130973E-14
9	Sub Reflector	262.8663	1.756615E-03	3.798051E-09	1.160802E-14
10	DODC Converter	263.8742	1.763420E-03	3.708442E-09	1.357872E-14
11	RF Shelf	263.9671	1.752322E-03	4.039884E-09	9.326652E-15
12	Det. Pre-Amp	263.4358	1.750480E-03	3.754149E-09	1.171233E-14
13	Warm Load Ctr	254.7616	1.653192E-03	5.988277E-09	3.101395E-14
14	Warm Load # 1	254.5737	1.652519E-03	5.994369E-09	3.214458E-14
15	Warm Load #2	254.6311	1.658779E-03	6.059266E-09	3.010172E-14
16	Warm Load #3	254.8459	1.655427E-03	6.099508E-09	3.020449E-14
17	Warm Load #4	254.8488	1.652000E-03	6.055910E-09	3.032410E-14
18	Warm Load #5	254.7966	1.647523E-03	6.068692E-09	2.974657E-14
19	Warm Load #6	253.9048	1.657694E-03	5.929873E-09	3.021740E-14

A.2 *Warm Load Correction*

The in-flight warm load correction (WLC) was calculated according to a formula developed by Aerojet [6-9]. For each AMSU-A antenna system, a special set of calibration data were acquired by setting the temperature of its variable scene target equal to that of the internal blackbody (warm) target. The physical temperature T_W of the internal blackbody target was determined from the PRT counts as described in Section 2. The radiometric temperature T_{wrad} of the blackbody (in-flight warm load) was calculated (for each scan in the data set) by the formula

$$T_{wrad} = T_{sprt} + \left(T_{sprt} - T_C\right)\left(\frac{C_W - C_S}{C_S - C_C}\right) \tag{A-3}$$

where: T_{sprt} = PRT temperature of the variable scene target,
T_C = PRT temperature of the cold target,
C_W = the average of two radiometric counts from the warm target,
C_C = the average of two radiometric counts from the cold target, and
C_S = radiometric counts from the variable scene target.

One should note that temperatures, T_{sprt} and T_C, from the scene and cold targets are used as the two reference calibration points in Equation (A-3) to calculate the radiometric temperature of the warm target. The in-flight warm load correction factor ΔT_W was computed from the formula,

$$\Delta T_W = \frac{1}{N}\left[\sum_{i=1}^{N}\left(T_{wrad} - T_W\right)_i\right] \tag{A-4}$$

where N represents the number of scans in the data set. The ΔT_W values at three instrument (RF Shelf) temperatures for each AMSU-A antenna system are listed in Table A-3. For AMSU-A1, the ΔT_W values for both PLLO#1 and PPLO#2 were calculated and listed. These ΔT_W values will be used in NOAA-N AMSU-A operational calibration algorithm.

A.3 *Nonlinearity parameters*

The nonlinearity is discussed in Section 4.2 and the values of the nonlinearity parameter u are listed in Table 4.

Table A-3. NOAA-N AMSU-A warm load corrections (K) at three instrument temperatures.

AMSU-A2 S/N 105 channels: **AMSU-A1-2 S/N 109 channels:**

Instrument Temp.(C)	Ch.1	Ch.2	Instrument Temp.(C)	Ch.3	Ch.4	Ch.5	Ch.8
-6.24	0.169	0.025	-2.35	-0.293	-0.131	-0.126	-0.173
12.18	0.125	0.046	18.30	0.016	-0.159	-0.092	-0.225
30.66	0.066	0.019	38.26	-0.107	-0.222	-0.240	-0.265

AMSU-A1-1 S/N 109 channels: PLLO#1:

Instrument Temp.(C)	Ch.6	Ch.7	Ch.9	Ch.10	Ch.11	Ch.12	Ch.13	Ch.14	Ch.15
-2.33	0.482	0.447	0.445	0.441	0.449	0.462	0.467	0.510	0.434
18.26	0.227	0.243	0.232	0.241	0.219	0.249	0.226	0.206	0.215
38.18	0.296	0.266	0.268	0.281	0.272	0.258	0.195	0.295	0.213

AMSU-A1-1 S/N 109 channels: PLLO#2:

Instrument Temp.(C)	Ch.9	Ch.10	Ch.11	Ch.12	Ch.13	Ch.14
-2.41	0.098	0.100	0.109	0.124	0.146	0.139
18.19	0.322	0.324	0.348	0.326	0.324	0.334
38.17	0.380	0.387	0.365	0.388	0.352	0.378

A.4 *Correction to In-orbit Cold Space Calibration*

For on-orbit cold space calibration, there is an uncertainty due to antenna side lobe interference with the Earth limb and spacecraft. The contribution from this uncertainty should be added to the cold space cosmic background temperature of 2.73K. Therefore, the "effective " cold space temperature T_{EC} can be represented by

$$T_{EC} = 2.73 + \Delta T_C \tag{A-5}$$

where ΔT_C represents the contribution due to antenna side lobe interference with the Earth limb and spacecraft. Aerojet made estimates of ΔT_C for individual channels and its values for NOAA-N AMSU-A [6, 7] are listed in Table A-4. These ΔT_C values will be used initially and the final optimal values for ΔT_C will be determined from the antenna pattern corrections [10].

Table A-4. Values of NOAA-N AMSU-A ΔT_C and limits of blackbody count variations.

Channel	ΔT_C (K)	ΔC_W (count)
1	0.46	15
2	0.58	19
3	1.46	12
4	1.46	11
5	1.65	15
6	1.22	8
7	1.25	8
8	1.68	11
9	1.22	10
10	1.22	10
11	1.22	14
12	1.22	18
13	1.22	25
14	1.22	42
15	1.18	3

A.5 *Limit of Blackbody Counts Variation*

For each scan, the blackbody count C_W is the average of two samples. If the two samples of the blackbody differ by more than a pre-set limit of blackbody count variation ΔC_W, the data in the scan will not be used. The ΔC_W values for individual channels are listed in Table A-4. These ΔC_W values, which equal approximately 3σ (where σ is the standard deviation of the internal blackbody counts), are calculated from the TV calibration data.

A.6 *Pre-launch Determined Weight Factors w_k for the Internal Blackbody PRTs*

The weight factors w_k (see Equation 2) assigned to individual PRTs in the internal blackbody targets are listed in Table A-5. All NOAA-N AMSU-A PRTs are good.

Table A-5. Pre-launch determined weight factors w_k assigned to NOAA-N AMSU-A PRTs in blackbody targets.

Antenna System	w_1	w_2	w_3	w_4	w_5	w_6	w_7
AMSU-A2	1	1	1	1	1	1	1
AMSU-A1-1	1	1	1	1	1		
AMSU-A1-2	1	1	1	1	1		

A.7 *Conversion Coefficients of Analog Data*

AMSU-A instrument has an analog telemetry bus to monitor key temperatures and voltages through the spacecraft. The resolutions of the analog telemetry received on the ground is 20 mV for one part in 256. To convert the analog data into physical quantities y, one must multiply the analog values by 0. 02V (20 mV) to obtain the measured output, x, in volts and then uses the conversion equation,

$$y = B + M x \tag{6}$$

where the values of B and M are given in Tables A-6 and A-7 for NOAA-N AMSU-A.

Table A-6. NOAA-N AMSU-A2 S/N 105: Analog data conversion coefficients.

UIIS	Description	y	M	B
1	Scanner Motor Temperature	c	68.027	0
2	Comp Motor Temperature	c	68.027	0
3	R.F. Shelf Temperature	c	68.027	0
4	Warm Load Temperature	c	68.027	0
5	Comp. Motor Current (average)	mA	46.6	0
6	Ant Drive Motor Current (ave)	mA	46.6	0
7	Signal Processing +15Vdc	v	4.315	0
8	Antenna Drive +15Vdc	v	4.315	0
9	Signal Processing -1 5Vdc	v	2.504	-22.562
10	Antenna Drive - 15Vdc	V	2.504	-22.562
11	Mixer/IF Amplifier +10 Vdc	V	2.889	0
12	Signal Processing +5Vdc	V	1.667	0
13	Antenna Drive +5Vdc	V	1.667	0
14	Local Oscillator +lOVdc. (ch.1)	V	2.861	0
15	Local Oscillator +lOVdc (ch.2)	V	2.861	0

Table A-7. NOAA-N AMSU-A1 S/N 109: Analog data conversion coefficients.

Spacecraft Connector P6 - Pin#	Description	y	m	b
3	A1-1 Scanner Motor Temperature	C	68.027	0
22	A1-2 Scanner Motor Temperature	C	68.027	0
2	A1-1 RF Shelf Temperature	C	68.027	0
21	A1-2 RF Shelf Temperature	C	68.027	0
4	A1-1 Warm Load Temperature	C	68.027	0
23	A1-2 Warm Load Temperature	C	68.027	0
8	A1-1 Antenna Drive Motor Current	mA	23.3	0
27	A1-2 Antenna Drive Motor Current	mA	23.3	0
11	Signal Processing (+15VDC)	V	4.315	0
9	Antenna Drive (+15 VDC)	V	4.315	0
29	Signal Processing (-15 VDC)	V	2.504	-22.562
28	Antenna Drive (-15 VDC)	V	2.504	-22.562
34	Receiver Amplifiers (+8 VDC)	V	2.5	0
12	Signal Processing (+5 VDC)	V	1.667	0
10	Antenna Drive (+5 VDC)	V	1.667	0
17	Receiver Mixer/IF (+10 VDC)	V	2.889	0
16	Phase Lock Loop Ch 9/14 (+15 VDC)	V	4.315	0
33	Phase Lock Loop Ch 9/14 (-15VDC)	V	2.504	-22.562
13	Ch 3 L.O. Voltage (50.3 GHz)	V	2.861	0
30	Ch 4 L.O. Voltage (52.8 GHz)	V	2.861	0
14	Ch 5 L.O. Voltage (53.596 GHz)	V	2.861	0
31	Ch 6 L.O. Voltage (54.4 GHz)	V	2.861	0
15	Ch 7 L.O. Voltage (54.94 GHz)	V	2.861	0
32	Ch 8 L.O. Voltage (55.5 GHz)	V	2.861	0
25	PLLO Primary Lock Detect (PLO #1)		1	0
6	PLLO Redundant Lock Detect (PLO #2)		1	0
18	Ch 15 L.O. Voltage (89.0 GHz)		4.315	0

mA = milliamps

APPENDIX B

NOAA-N' CPIDS : COEFFICIENTS OF AMSU-A1 S/N 105 AND AMSU-A2 S/N 107

In this appendix, the NOAA-N' AMSU-A CPIDS are presented in a similar fashion as those for NOAA-N AMSU-A given in the main text and Appendix A. Tables of coefficients and plots of results from analysis of the TV calibration data follow the same order as that of NOAA-N calibration steps as closely as possible. The NOAA-N' analog conversion coefficients are identical to those of NOAA-N (Tables A-6 and A-7).

Table B-1. NOAA-N' channel characteristics and specifications (AMSU-A1 S/N 105 and A2 S/N 107).

Channel	Channel Frequency (MHz)		No. of	Measured 3-dB RF Bandwidth	NEDT (K)		Beam #	Polarization	FOV**
Number	Specification	Measured *	Bands	(MHz)	Spec.	Measured	Efficiency	(NADIR)	(deg.)
1	23800	23800.37	1	251.02	0.30	0.191	96%	V	3.50
2	31400	31401.72	1	160.32	0.30	0.214	97%	V	3.34
3	50300	50300.63	1	160.88	0.40	0.220	96%	V	3.45
4	52800	52800.00	1	379.68	0.25	0.130	96%	V	3.37
5	53596 ± 115	53596.29 ± 115	2	167.71 | 167.71	0.25	0.148	96%	H	3.40
6	54400	54399.86	1	380.10	0.25	0.146	97%	H	3.38
7	54940	54940.68	1	380.18	0.25	0.147	97%	V	3.41
8	55500	55500.36	1	309.98	0.25	0.156	96%	H	3.32
9	fo = 57290.344	fo = 57290.340	1	310.08	0.25	0.152	97%	H	3.31
10	fo ± 217	fo ± 217	2	76.24 | 76.24	0.40	0.200		H	
11	fo ± 322.2 ± 48	fo ± 322.2 ± 48	4	34.85 / 35.33 | 35.33 / 34.85	0.40	0.225		H	
12	fo ± 322.2 ± 22	fo ± 322.2 ± 22	4	15.43 / 15.48 | 15.48 / 15.43	0.60	0.318		H	
13	fo ± 322.2 ± 10	fo ± 322.2 ± 10	4	7.82 / 7.88 | 7.88 / 7.82	0.80	0.460		H	
14	fo ± 322.2 ± 4.5	fo ± 322.2 ± 4.5	4	2.94 / 2.95 | 2.95 / 2.94	1.20	0.735		H	
15	89000	88998.50	1	1987.38	0.50	0.129	99%	V	3.42

* At temperature 22 degree C. ** Specification is required to have 3.3 degrees ± 10% for all channels # Measured.

Table B-2. NOAA-N' nonlinearity parameters u in dimension of (m^2-sr-cm^{-1})/mW.

AMSU-A2 S/N 107 channels: **AMSU-A1-2 S/N 105 channels:**

Instrument Temp.(C)	Ch.1	Ch.2	Instrument Temp.(C)	Ch.3	Ch.4	Ch.5	Ch.8
-7.51	5.253912	1.747521	-1.86	0.102041	1.001680	0.644706	0.575094
11.54	6.514634	2.098065	18.03	0.160760	0.985232	0.647093	0.540837
30.28	5.567306	2.135754	38.49	0.144439	0.955517	0.675383	0.590397

AMSU-A1-1 S/N 105 channels: PLLO#1

Instrument Temp.(C)	Ch.6	Ch.7	Ch.9	Ch.10	Ch.11	Ch.12	Ch.13	Ch.14	Ch.15
-2.15	2.306031	2.052798	2.337700	2.476749	2.118502	2.182972	2.201144	2.313345	0.754824
17.70	2.903638	2.477733	2.674379	2.840808	2.341382	2.411666	2.365599	2.456567	0.901620
38.48	2.563713	2.343362	2.529602	2.203366	2.152229	2.208964	2.162437	2.250723	0.852319

AMSU-A1-1 S/N 105 channels: PLLO#2

Instrument Temp.(C)	Ch.9	Ch.10	Ch.11	Ch.12	Ch.13	Ch.14
-2.41	2.246910	2.386747	1.982684	2.088893	1.980516	0.990261
18.23	2.496602	2.555799	2.245905	2.309513	2.277664	0.945647
38.35	2.491529	2.314953	2.101398	2.174355	2.232316	0.850793

Table B-3. NOAA-N' AMSU-A warm load corrections (K) at three instrument temperatures.

AMSU-A2 S/N 107 channels: **AMSU-A1-2 S/N 105 channels:**

Instrument Temp.(C)	Ch.1	Ch.2	Instrument Temp.(C)	Ch.3	Ch.4	Ch.5	Ch.8
-7.51	0.092	0.084	**-2.35**	0.095	0.027	0.034	0.031
11.54	-0.053	-0.041	**18.30**	0.242	0.000	-0.014	0.014
30.28	-0.161	-0.123	**38.26**	-0.022	-0.090	-0.093	-0.095

AMSU-A1-1 S/N 105 channels: PLLO#1:

Instrument Temp.(C)	Ch.6	Ch.7	Ch.9	Ch.10	Ch.11	Ch.12	Ch.13	Ch.14	Ch.15
-2.15	0.324	0.385	0.312	0.242	0.348	0.302	0.291	0.288	0.308
17.70	0.311	0.380	0.321	0.228	0.326	0.315	0.319	0.329	0.304
38.48	0.112	0.092	0.078	-0.091	0.084	0.080	0.077	0.087	0.060

AMSU-A1-1 S/N 105 channels: PLLO#2:

Instrument Temp.(C)	Ch.9	Ch.10	Ch.11	Ch.12	Ch.13	Ch.14
-2.41	0.241	0.147	0.253	0.213	0.181	0.222
18.19	0.180	0.114	0.192	0.190	0.198	0.214
38.17	0.214	0.198	0.237	0.228	0.266	0.190

Table B-4. NOAA-N' AMSU-A1 S/N 105: Polynomial coefficients for converting PRT counts into temperatures.

PRT No.	Description	Fk0 (K)	Fk1 (K/count)	Fk2 (K/count^2)	Fk3 (K/count^3)
1	Al-1 MOTOR	263.4701	1.763558E-03	3.874897E-09	1.054742E-14
2	A1-2 MOTOR	263.0199	1.766179E-03	3.846105E-09	1.088355E-14
3	Al-1 Feed Horn	262.7290	1.762554E-03	3.871840E-09	1.116472E-14
4	A1-2 Feed Horn	261.4394	1.752306E-03	4.092637E-09	7.828227E-15
5	Al-1 RFMUX	263.2667	1.762355E-03	3.892085E-09	1.080806E-14
6	Al-2 RFMUX	263.5250	1.765351E-03	3.780640E-09	9.678754E-15
7	Ch. 3 DRO	263.2579	1.765074E-03	3.811636E-09	1.199675E-14
8	CH. 4 DRO	263.1725	1.764826E-03	3.855985E-09	1.158644E-14
9	CH. 5 DRO	263.0934	1.750481E-03	4.148659E-09	1.154537E-14
10	CH. 6 DRO	263.2155	1.770631E-03	3.851457E-09	1.203102E-14
11	CH. 7 DRO	263.2366	1.764003E-03	3.871023E-09	1.108513E-14
12	CH. 8 DRO	263.5302	1.768619E-03	3.875152E-09	1.188343E-14
13	CH. 15 GDO	264.0388	1.780004E-03	3.640650E-09	8.828566E-15
14	CH.9-14 PLO#2	263.8667	1.769988E-03	3.834479E-09	1.045077E-14
15	CH.9-14 PLO#1	263.6049	1.774948E-03	3.590613E-09	1.186157E-14
16	NOT used	263.6049	1.774948E-03	3.590613E-09	1.186157E-14
17	CH. 3 Mixer/IF	263.0478	1.745731E-03	4.857510E-09	-3.571623E-15
18	CH. 4 Mixer/IF	263.6584	1.768911E-03	3.765121E-09	1.115634E-14
19	CH. 5 Mixer/IF	263.4210	1.766045E-03	3.843205E-09	1.092880E-14
20	CH. 6 Mixer/IF	262.9807	1.774180E-03	3.881552E-09	1.096134E-14
21	CH. 7 Mixer/IF	263.2282	1.766166E-03	3.891861E-09	1.109550E-14
22	CH. 8 Mixer/IF	264.0072	1.761032E-03	3.762147E-09	1.361707E-14
23	CH.9-14 Mixer/IF	263.8931	1.768899E-03	3.695761E-09	1.214041E-14
24	CH. 15 Mixer/IF	263.7784	1.763818E-03	3.826228E-09	1.209923E-14
25	CH.11-14 IF AMP	263.3042	1.779052E-03	3.824151E-09	1.242656E-14
26	CH. 9 IF AMP	262.8711	1.758869E-03	3.905955E-09	1.001020E-14
27	CH. 10 IF AMP	263.7085	1.766714E-03	3.720646E-09	1.380529E-14
28	CH. 11 IF AMP	263.1634	1.766040E-03	3.807795E-09	1.234029E-14
29	DC/DC converter	263.0175	1.765419E-03	3.821587E-09	1.213039E-14
30	CH. 13 IF AMP	262.9424	1.761553E-03	3.912995E-09	1.131355E-14
31	CH. 14 IF AMP	263.4557	1.769266E-03	3.817872E-09	1.176563E-14
32	CH. 12 IF AMP	263.4728	1.768170E-03	3.775658E-09	1.284009E-14
33	Al-1 RFSHELF	263.2035	1.764930E-03	3.938845E-09	8.887988E-15
34	A1-2 RFSHELF	263.3260	1.768109E-03	3.830533E-09	1.352790E-14
35	DET/PRE-AMP	263.0042	1.756051E-03	4.037257E-09	1.440049E-14
36	Al-1 warm load 1	254.5588	1.672560E-03	6.029413E-09	3.112716E-14
37	Al-1 warm load 2	254.2882	1.666196E-03	6.095935E-09	3.234955E-14
38	Al-1 warm load 3	254.2658	1.663835E-03	6.128539E-09	3.108911E-14
39	Al-1 warm load 4	254.8582	1.664005E-03	6.097433E-09	3.152553E-14
40	A1-1 wm LD center	254.5439	1.663158E-03	6.137348E-09	3.047658E-14
41	A1-2 warm load 1	254.1800	1.662935E-03	6.098733E-09	3.139438E-14
42	A1-2 warm load 2	254.4506	1.635177E-03	8.761748E-09	-2.820614E-14
43	A1-2 warm load 3	254.5427	1.660404E-03	6.116786E-09	3.085850E-14
44	A1-2 warm load 4	254.6386	1.661026E-03	6.189887E-09	2.978715E-14
45	A1-2 wm LD center	254.6086	1.671941E-03	6.009501E-09	3.090084E-14

Table B-5. NOAA-N' AMSU-A2 S/N 107: Polynomial coefficients for converting PRT counts into temperatures.

PRT No.	Description	Fk0 (K)	Fk1 (K/count)	Fk2 (K/count^2)	Fk3 (K/count^3)
1	Scan Motor	263.4044	1.742455E-03	3.802621E-09	8.830967E-15
2	Feedhorn	263.8239	1.736622E-03	3.839440E-09	9.382127E-15
3	RF Diplexer	263.6269	1.742366E-03	3.699821E-09	1.299038E-14
4	Mixer/IF CH1	262.9692	1.734181E-03	3.884284E-09	9.125286E-15
5	Mixer/IF CH2	263.1765	1.737744E-03	3.758182E-09	1.040305E-14
6	CH I DRO	263.2004	1.735575E-03	3.853613E-09	1.065068E-14
7	CH 2 DRO	263.2366	1.741032E-03	3.691869E-09	1.162538E-14
8	Compensat Motor	263.4945	1.733846E-03	4.031591E-09	4.564074E-15
9	Sub Reflector	263.5057	1.742102E-03	3.754963E-09	9.869434E-15
10	DODC Converter	263.4324	1.735051E-03	3.783136E-09	9.984160E-15
11	RF Shelf	262.6547	1.760077E-03	3.760405E-09	1.228728E-14
12	Det. Pre-Amp	263.4431	1.736341E-03	3.862723E-09	8.819797E-15
13	Warm Load Ctr	253.702	1.655934E-03	5.604876E-09	2.580310E-14
14	Warm Load # 1	254.4634	1.671111E-03	5.461466E-09	2.278010E-14
15	Warm Load #2	254.5032	1.644841E-03	5.801831E-09	2.851984E-14
16	Warm Load #3	254.6432	1.671112E-03	5.446864E-09	2.557504E-14
17	Warm Load #4	254.2714	1.662008E-03	5.563689E-09	2.451621E-14
18	Warm Load #5	254.3559	1.665351E-03	5.706320E-09	2.623082E-14
19	Warm Load #6	254.3639	1.669415E-03	5.526940E-09	2.473715E-14

NOAA-N': AMSU-A2 S/N 107 RF-Shelf Temperature (C): xx= -7.5, **=11.5, ++=30.3
AMSU-A1 S/N 105 RF-Shelf Temperature (C): xx= -2.0, **=17.9, ++=38.5

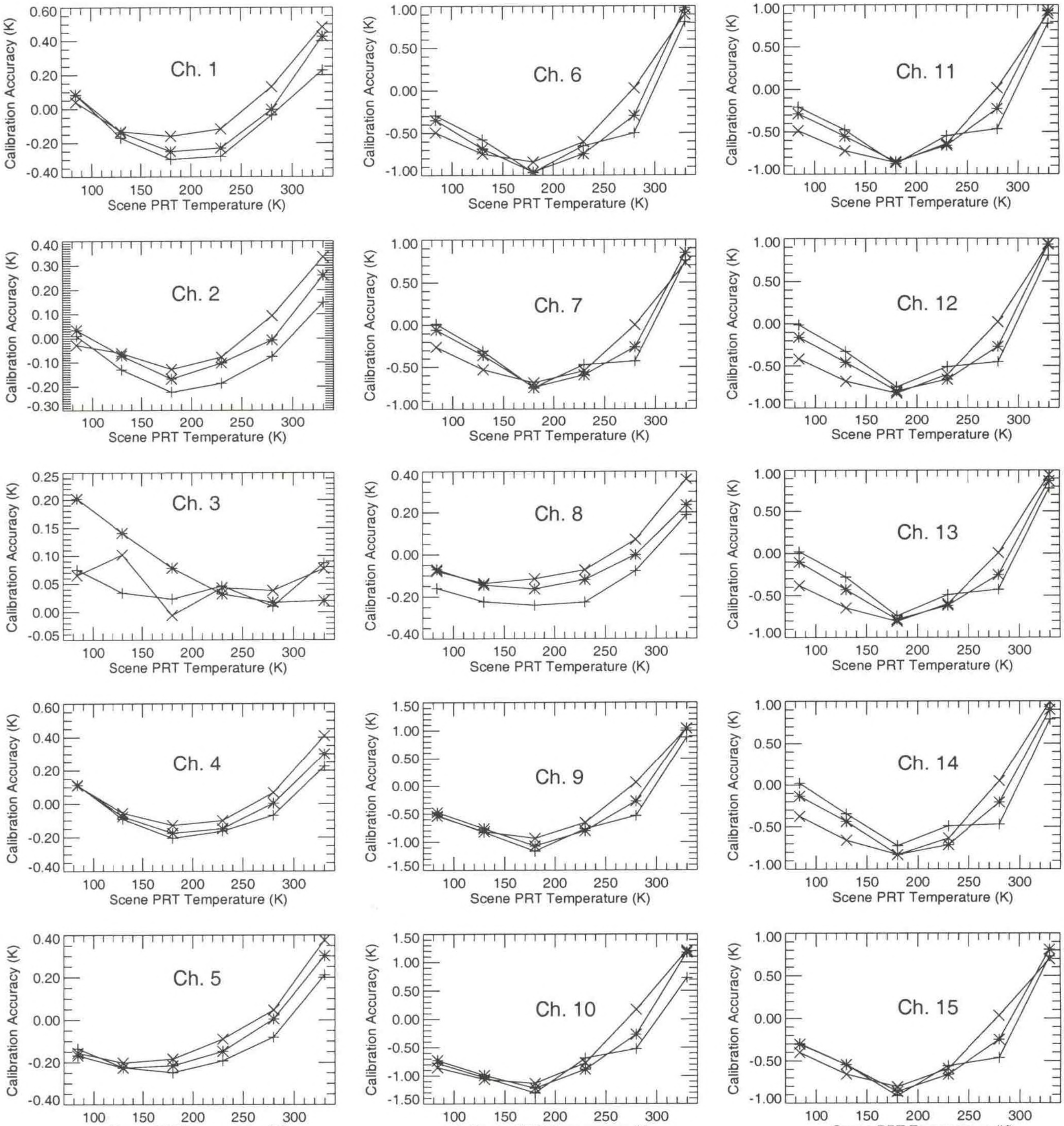

Figure B-1. NOAA-N' AMSU-A : Calibration accuracies at three instrument temperatures.

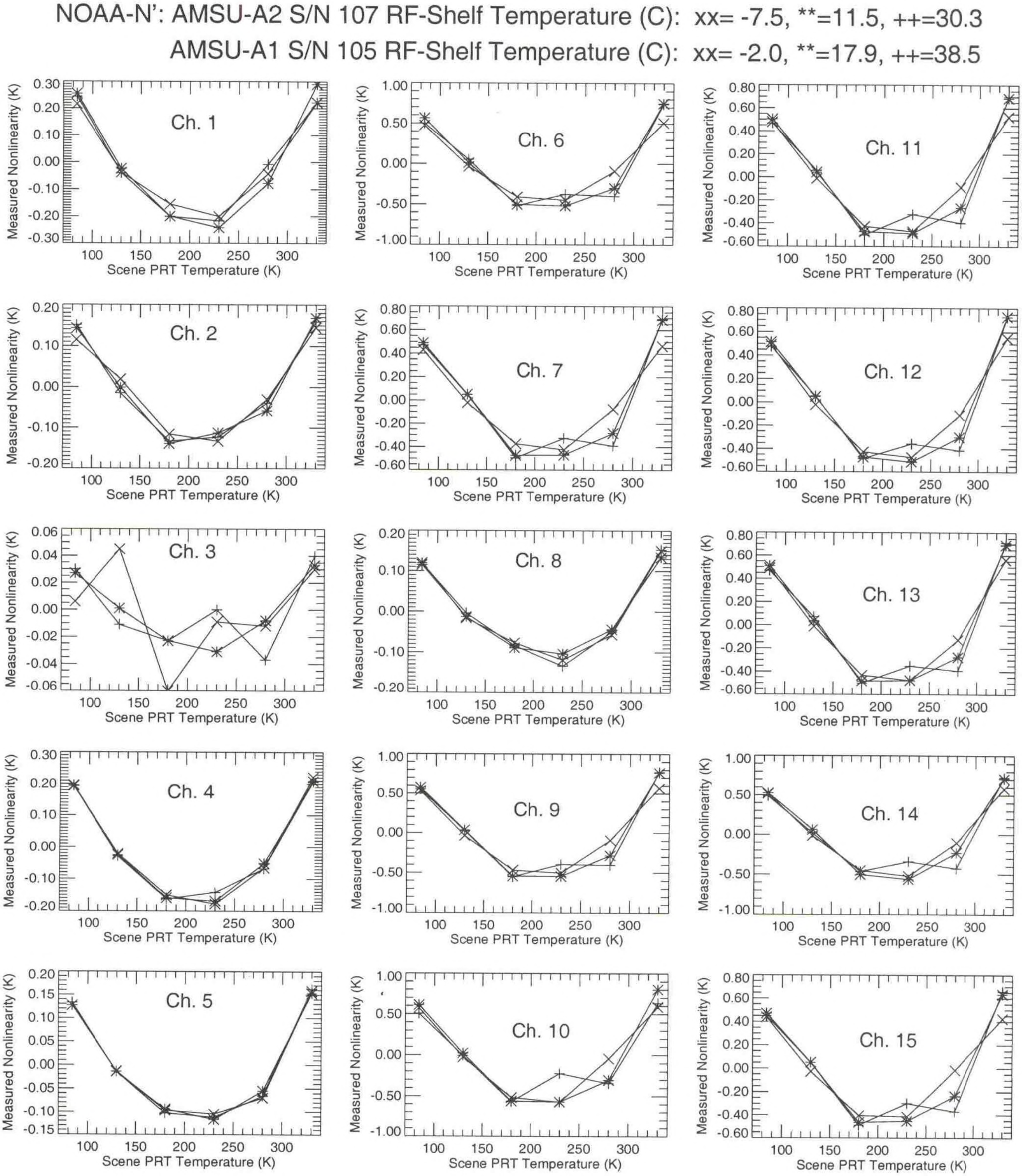

Figure B-2. NOAA-N' AMSU-A : Residuals after least-squares fit of the scene PRT radiance as a function of R_{SL} as discussed in the text.

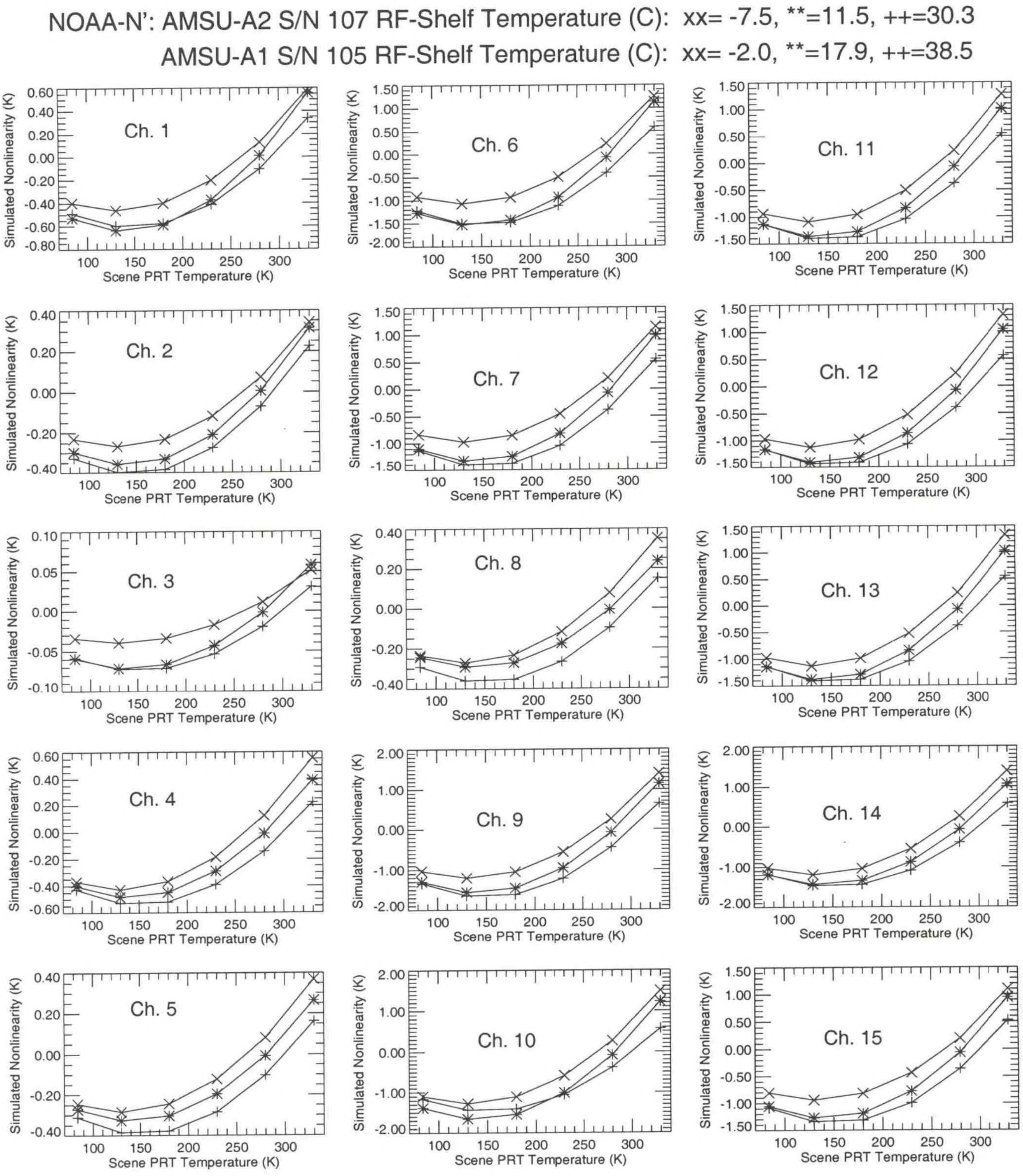

Figure B-3. NOAA-N' AMSU-A: Simulated nonlinear corrections which are expected from on-orbit data.

NOAA-N': AMSU-A2 S/N 107 RF-Shelf Temperature (C): xx= -7.5, **=11.5, ++=30.3
AMSU-A1 S/N 105 RF-Shelf Temperature (C): xx= -2.0, **=17.9, ++=38.5

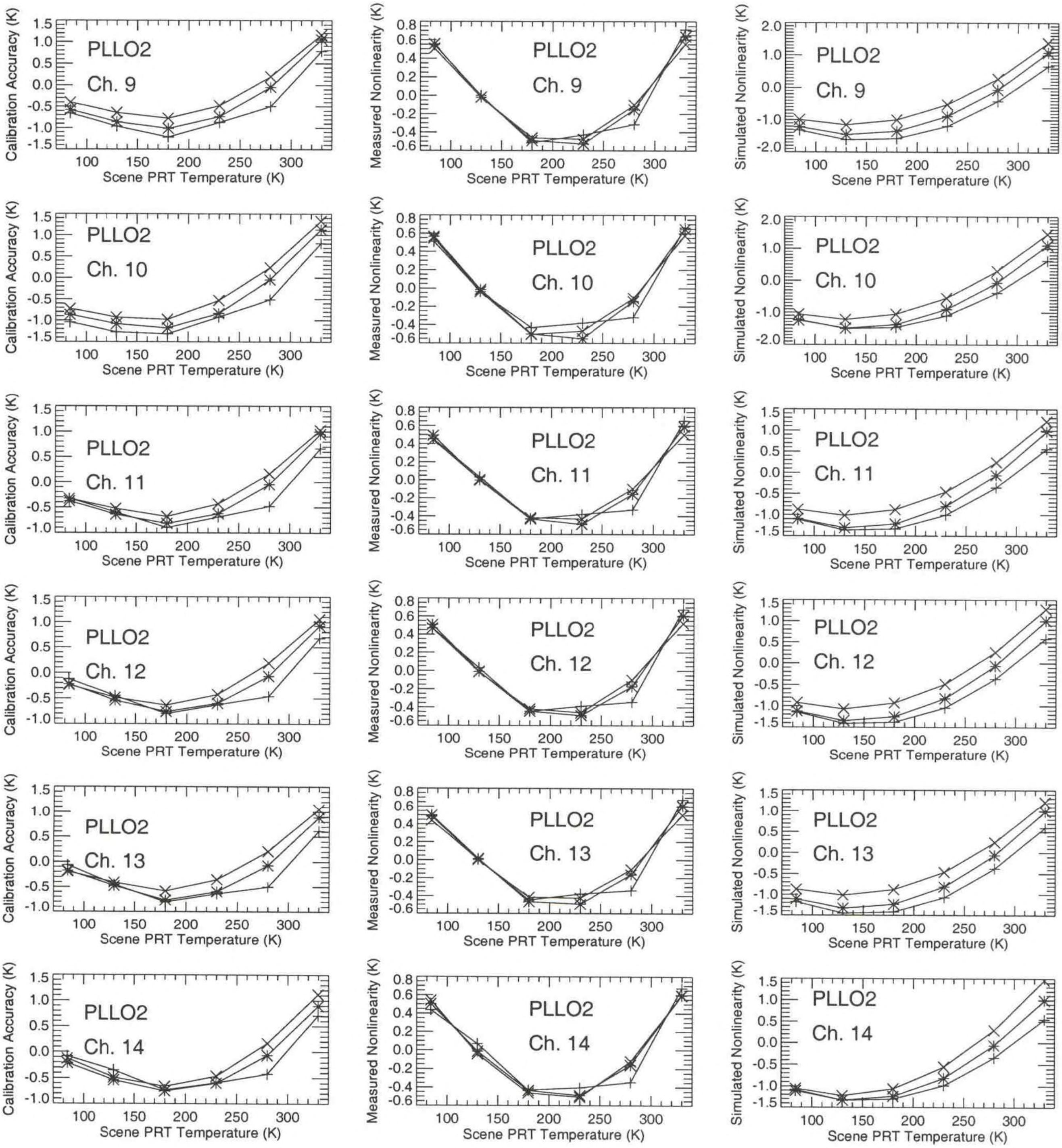

Figure B-4. NOAA-N' AMSU-A : Calibration results withe PLLO #2 in Channels 9-14,
(a) calibration accuracy, (b) measured nonlinearity, and (c) simulated nonlinearity.

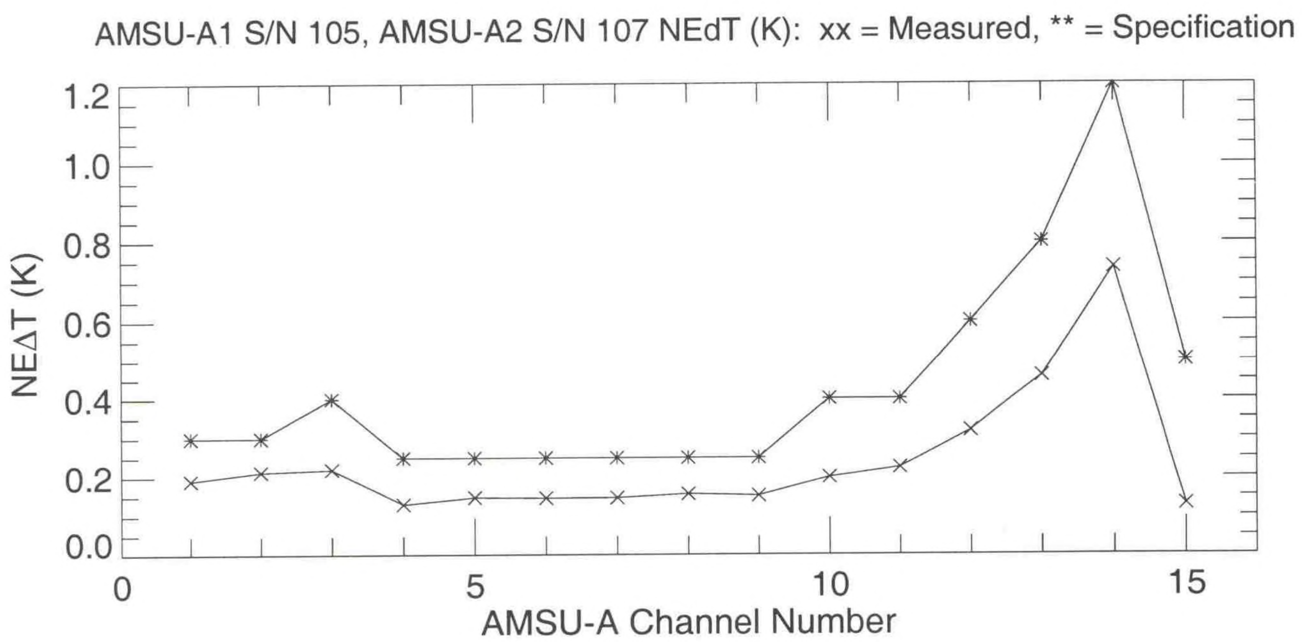

Figure B-5. NOAA-N' AMSU-A: Comparison of the measured NEΔT values with specification.

NOAA-N': AMSU-A2 S/N 107 RF-Shelf Temperature (C): xx= -7.5, **=11.5, ++=30.3
AMSU-A1 S/N 105 RF-Shelf Temperature (C): xx= -2.0, **=17.9, ++=38.5

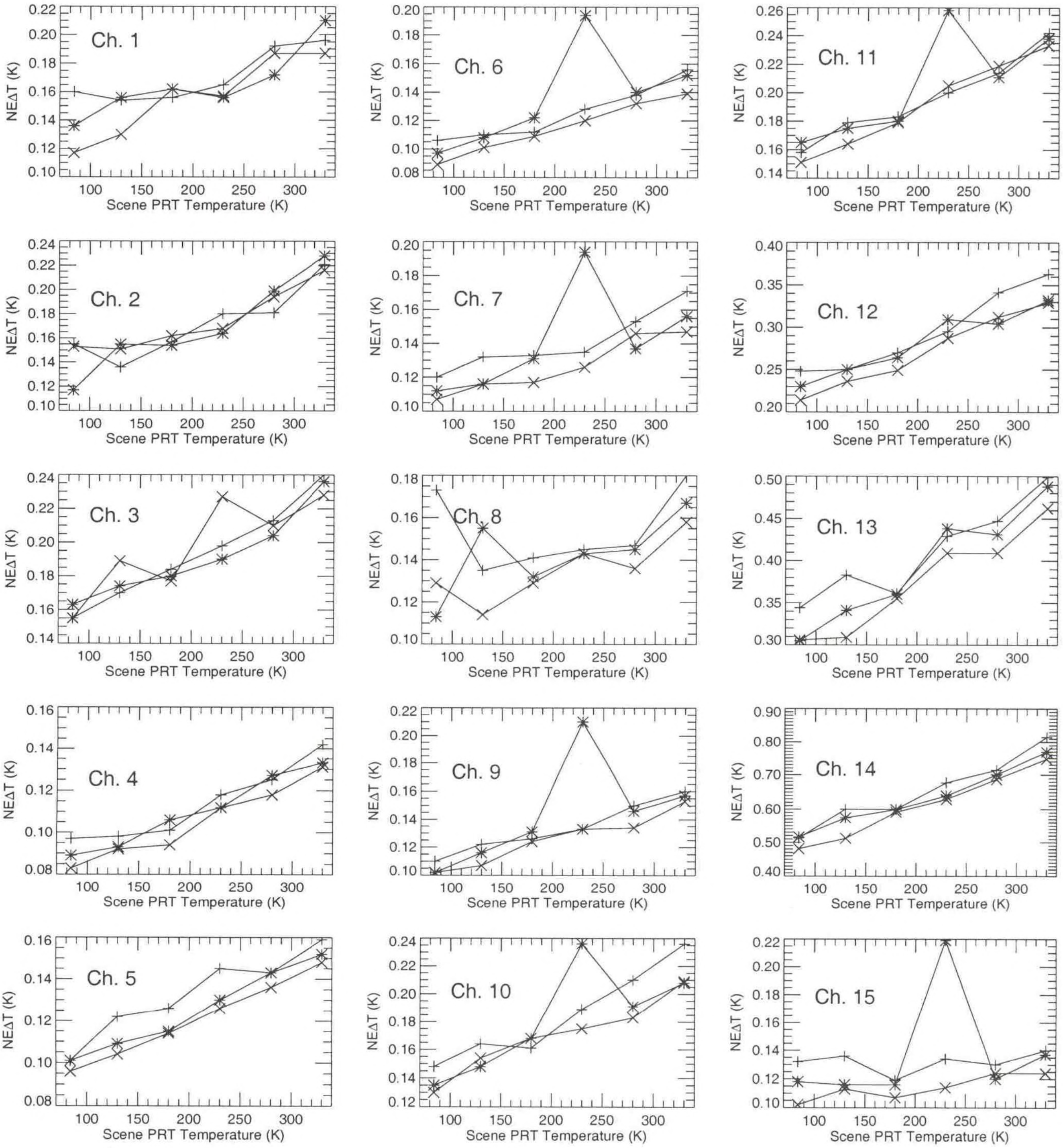

Figure B-6. NOAA-N' AMSU-A: Measured NEΔT values at three instrument temperatures.

NOAA-N': AMSU-A2 S/N 107 RF-Shelf Temperature (C): xx= -7.5, **=11.5, ++=30.3
AMSU-A1 S/N 105 RF-Shelf Temperature (C): xx= -2.0, **=17.9, ++=38.5

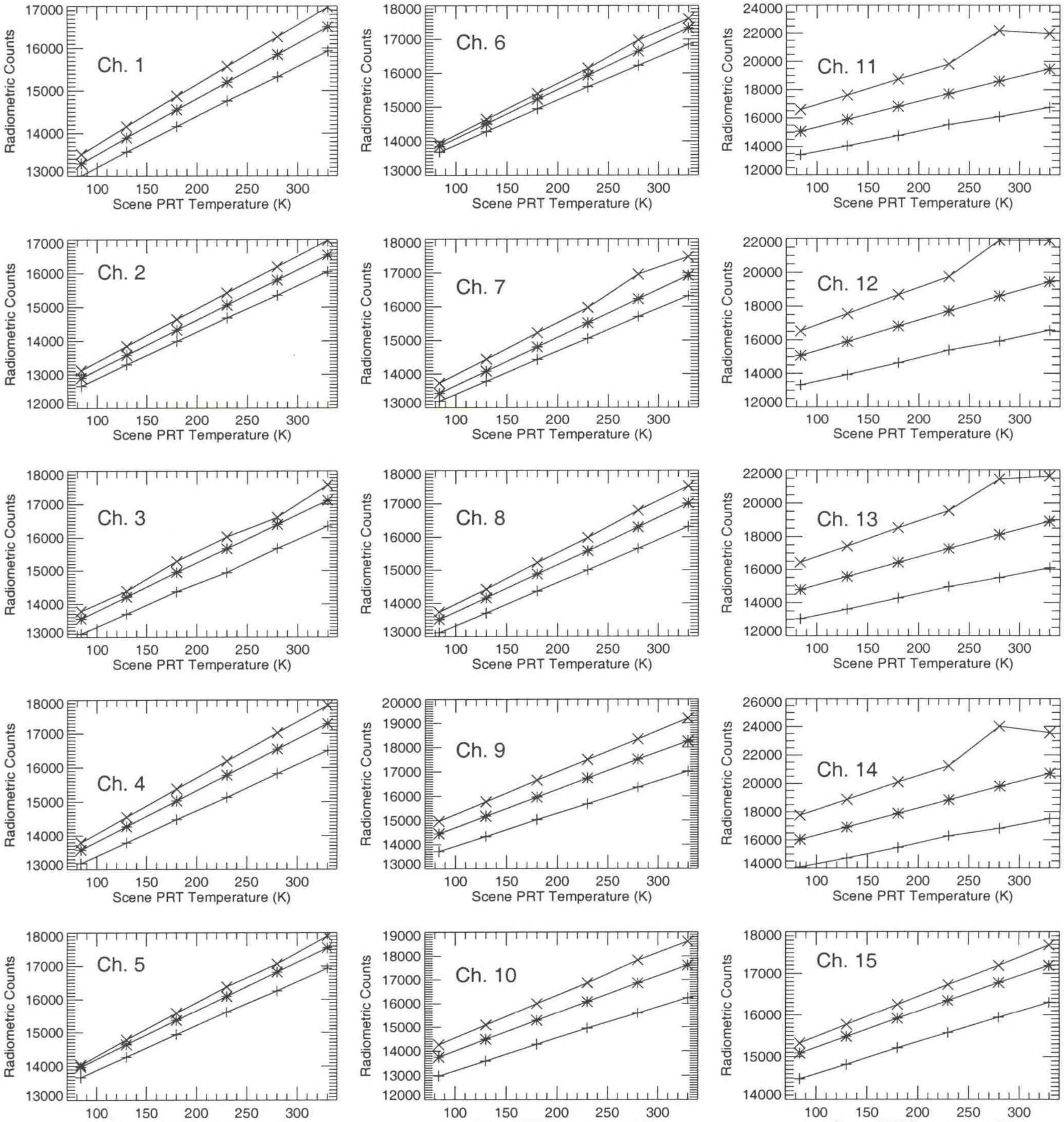

Figure B-7. NOAA-N' AMSU-A: Radiometric counts versus scene PRT temperature at three instrument temperatures.

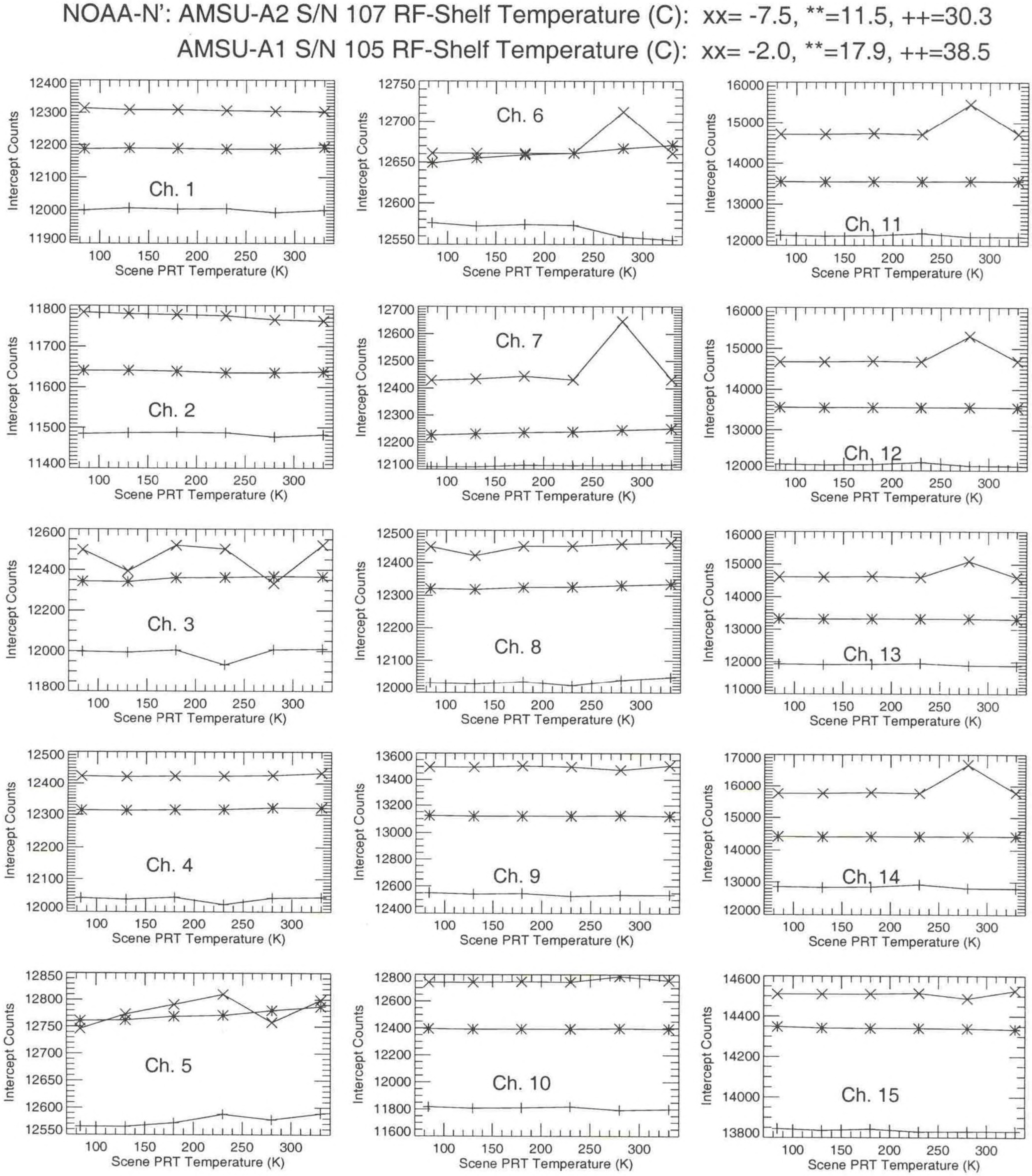

Figure B-8. NOAA-N' AMSU-A: Intercept counts at three instrument temperatures.

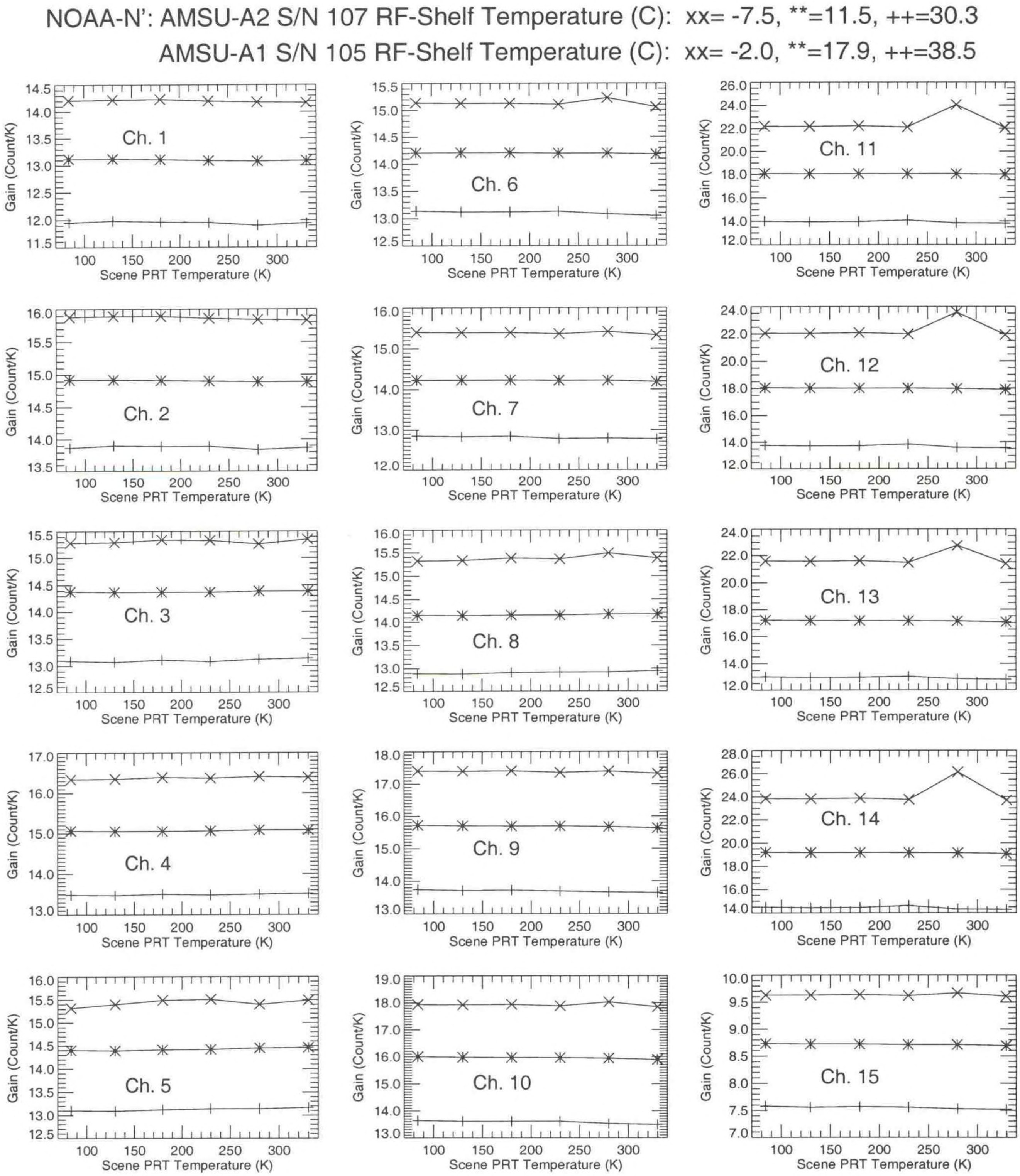

Figure B-9. NOAA-N' AMSU-A: Channel gains at three instrument temperatures.

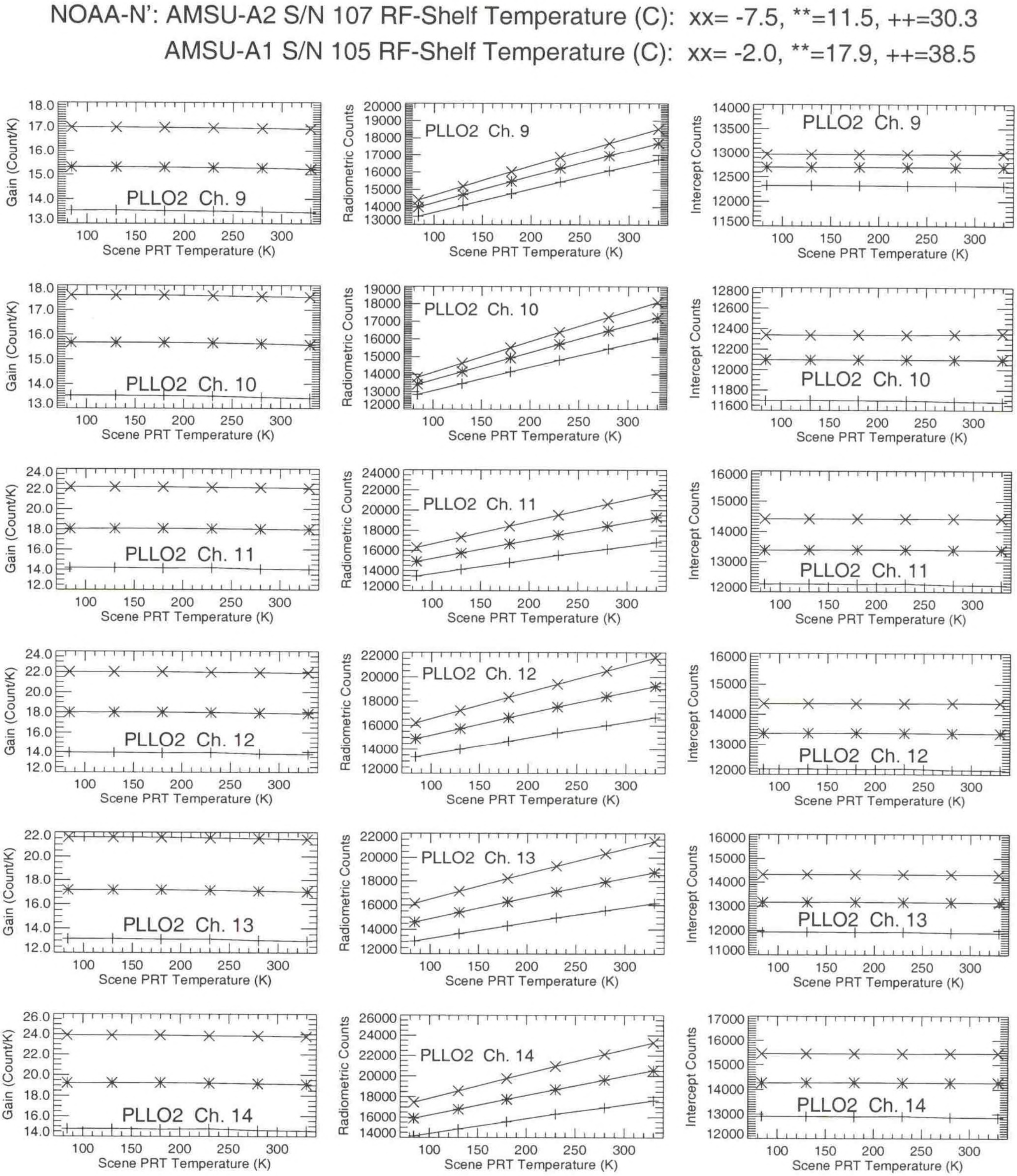

Figure B-10. NOAA-N' AMSU-A: Calibration results with PLLO #2, including gains, radiometric counts, and intercept counts at three instrument temperatures.

APPENDIX C

NOAA LEVEL 1B DATA AND SAMPLES OF AMSU-A ON-ORBIT DATA

The NOAA Polar Orbiter Level 1B data are raw data that have been quality controlled and assembled into discrete data sets, to which Earth location and calibration information are appended but not applied. For simplification of application, one can rewrite Equation (4) as,

$$R_S = a_0 + a_1 C_S + a_2 C_S^2 \tag{C-1}$$

where the calibration coefficients a_i (where i = 0, 1, and 2) can be expressed in terms of R_W, G, $\overline{C_W}$ and $\overline{C_C}$. This can be accomplished by rewriting the right-hand side of Equation (4) in powers of C_S and equates the a_i's to the coefficients of same powers of C_S. The results are,

$$a_0 = R_W - \frac{\overline{C}_W}{G} + u\frac{\overline{C}_W \overline{C}_C}{G^2} \tag{C-2}$$

$$a_1 = \frac{1}{G} - u\frac{\overline{C}_C + \overline{C}_W}{G^2} \tag{C-3}$$

and

$$a_2 = u\frac{1}{G^2} \tag{C-4}$$

These calibration coefficients will be calculated at each scan line for all channels and appended to the 1B data. With these coefficients, one can simply apply Equation (C-1) to obtain the scene radiance R_S. Users, who prefer brightness temperature instead of radiance, can make the simple conversion,

$$T_S = B^{-1}\left(R_S\right) \tag{C-5}$$

where $B^{-1}(R_S)$ is the inverse of the Planck function for radiance R_S. The T_S is the converted brightness temperature.

The coefficients defined in Equations (C-2) to (C-4) are functions of instrument temperature. In general, they are not constant and should be re-calculated at each scan. To demonstrate the dynamic features of the calibration coefficients, the a_0, a_1, and a_2 values calculated from one orbit of the

NOAA-16 AMSU-A 1B data are shown in Figure C-1. These time series of calibration coefficients show the changes over the period. Therefore, they must be calculated at each scan line and their values obtained from pre-launch data [6-9] can not be employed to convert the radiometric counts into temperatures.

Figure C-2 shows the instrument (RF Shelf) temperature variation during the same orbital period. It shows that RF Shelf temperature changed only about 2 K during the orbital period, but it is large enough to induce signification variation in the a_0, a_1, and a_2 coefficients. The RF Mux temperature, which is used as a backup instrument temperature, is also shown in Figure C-2. Similarly, the effect of the instrument temperature on the cold space and blackbody radiometric counts is also significant. These are shown in Figures C-3 and C-4, where the space and blackbody radiometric counts versus the scan line number are displayed. The variations in the space and warm radiometric counts are mainly due to changes in the instrument temperatures. Analysis of these NOAA-16 AMSU-A on-orbit data provides us with a better understanding of the AMSU-A instrument performance in space and helps process the pre-launch calibration data.

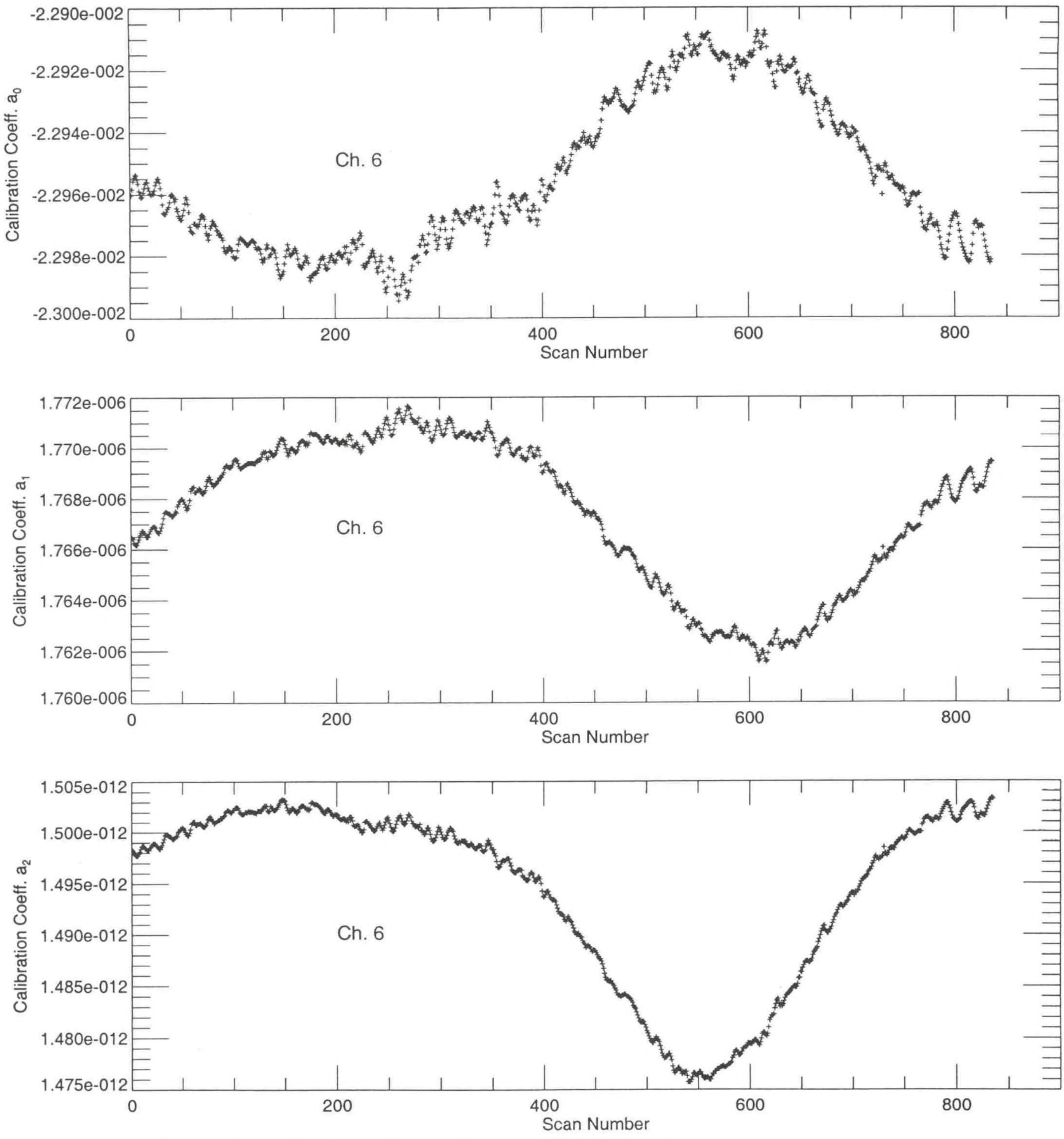

Figure C-1. NOAA-16 AMSU-A on-orbit data : Calibration coefficients, a_0, a_1, and a_2 values at Channel 6 over one orbit.

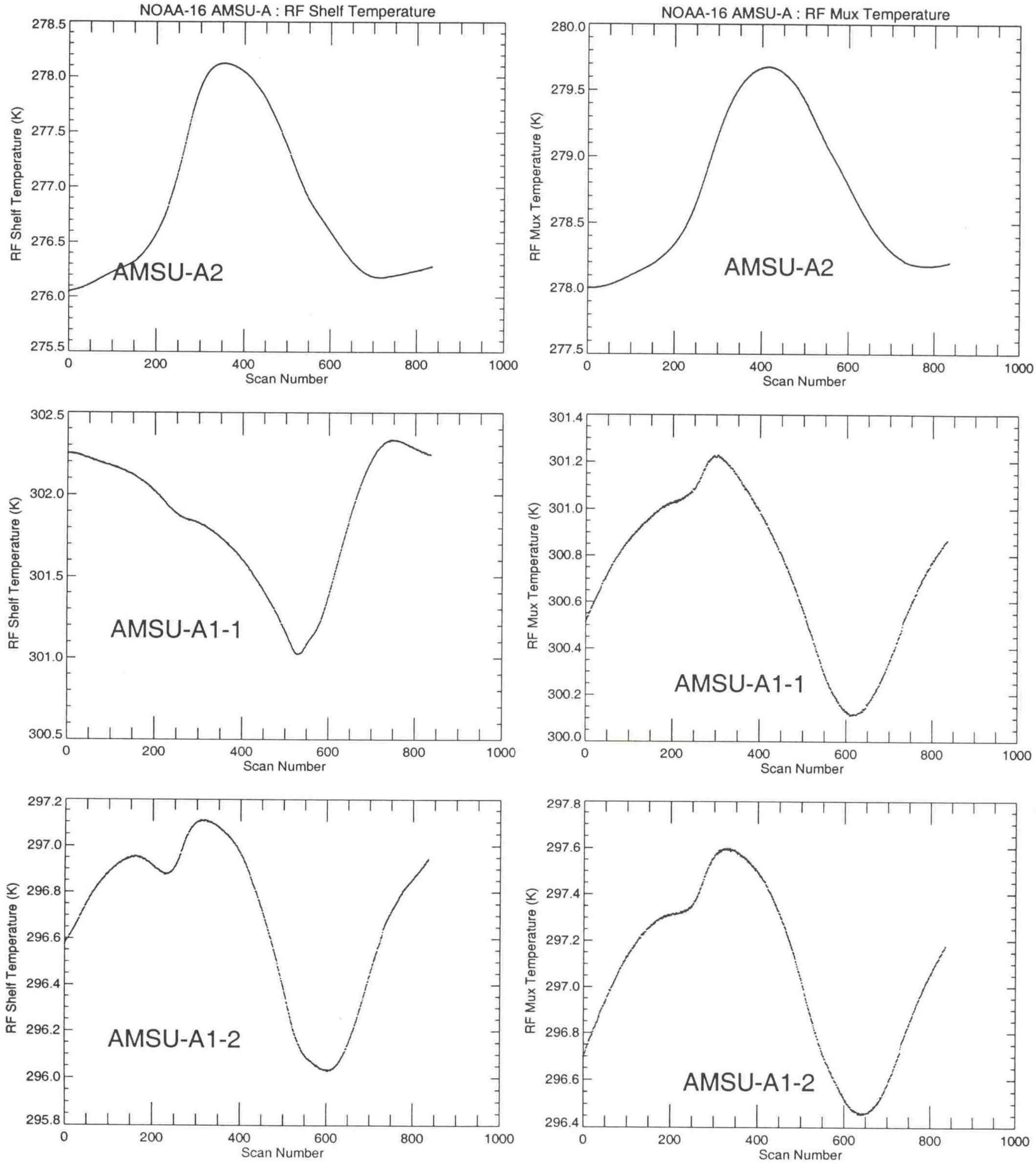

Figure C-2. NOAA-16 AMSU-A on-orbit data: RF-Shelf and RF Mux temperatures over one orbital period.

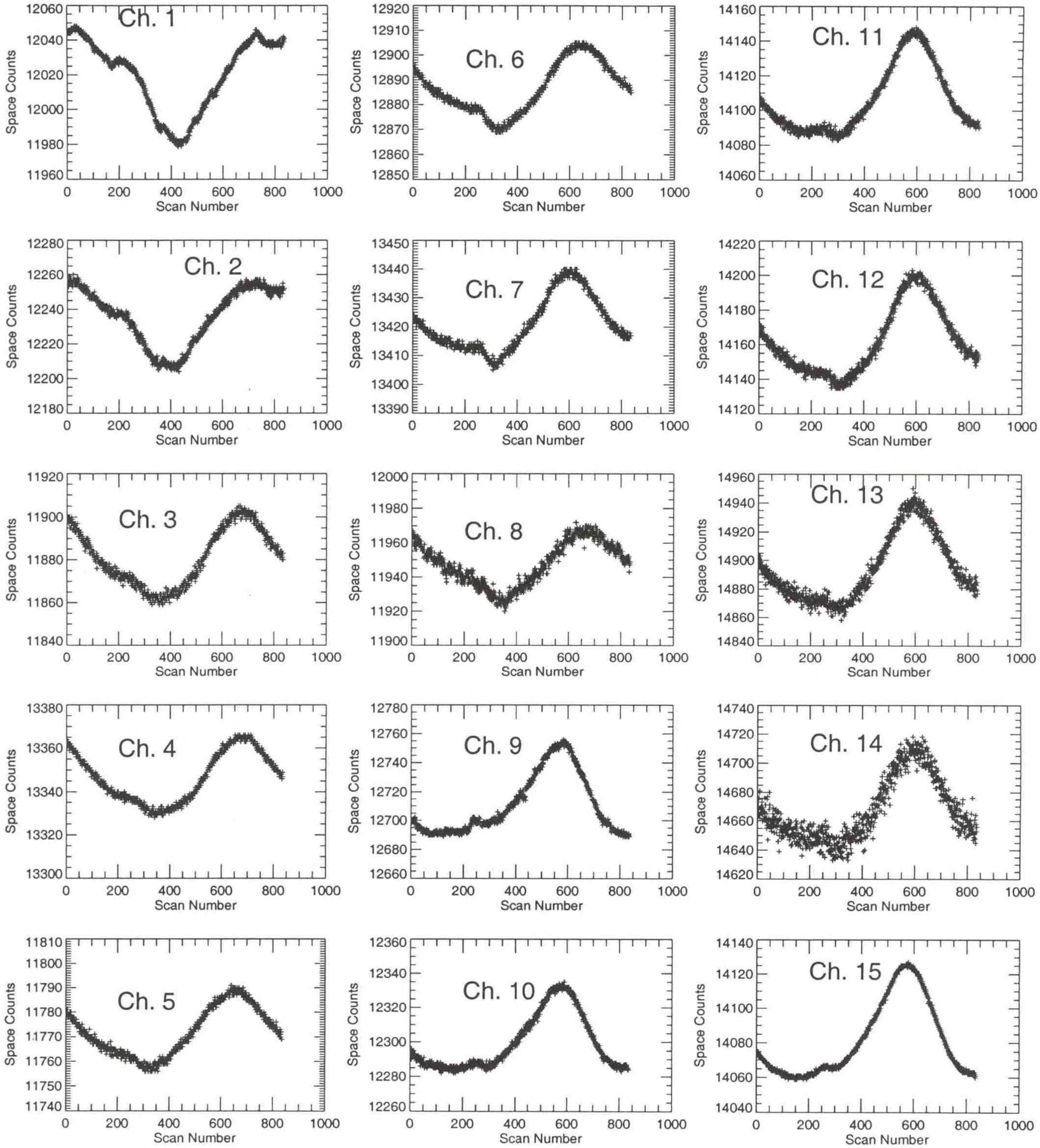

Figure C-3. NOAA-16 AMSU-A on-orbit data: Radiometric space counts over one orbital period.

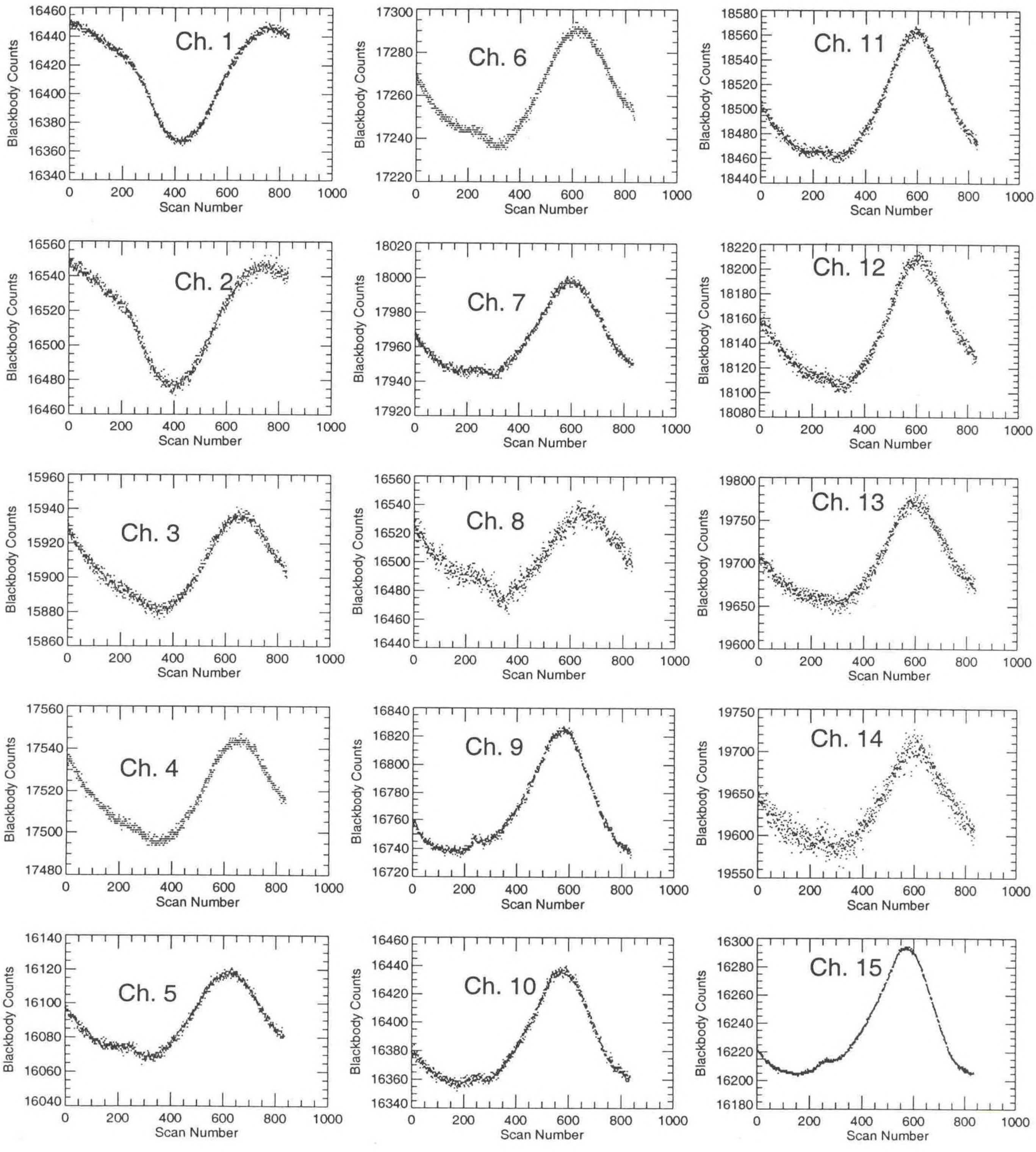

Figure C-4. NOAA-16 AMSU-A on-orbit data: Radiometric blackbody counts over one orbital period.

NESDIS 81 Quality Control and Processing of Historical Oceanographic Temperature, Salinity, and Oxygen Data. Timothy Boyer and Sydney Levitus, August 1994.

NESDIS 82 An Introduction to the GOES I-M Imagr and Sounder Instruments and the GVAR Retransmission Format. Raymond Komajda (Mitre Corp), November 1994.

NESDIS 83 Tropical Cyclone Motion Forecasting Using Satellite Water Vapor Imagery. Vernon F. Dvorak and H. Michael Mogil, December 1994.

NESDIS 84 Spurious Semi-Diurnal Variation in the E.R.B.E. Outgoing Longwave Radiation. C. R. Kondragunta and Arnold Gruber, June 1995.

NESDIS 85 Calibration of the Advanced Microwave Sounding Unit-A for NOAA-K. Tsan Mo, June 1995.

NESDIS 86 A Spectral approach to the Forward Problem in GPS Radio Occulation Remote Sensing (Ray Tracing, Assimilation, Tomography). Simon Rosenfeld, July 1996.

NESDIS 87 Proceedings of the International Workshop on Oceanographic Biological and Chemical Data Management. Sponsors Intergovernmental Oceanographic Commission, U.S. National Oceanographic Data Center, European Union MAST Programme, May 1996.

NESDIS 88 Analytical Model of Refraction in a Moist Polytropic Atmosphere for Space and Ground-Based GPS Applications. Simon Rosenfeld, April 1997.

NESDIS 89 A GOES Image Quality Analysis System for the NOAA/NESDIS Satellite Operations Control Center. Donald H. Hillger and Peter J. Celone, December 1997.

NESDIS 90 Automated Satellite-Based Estimates of Precipitation: An Assessment of Accuracy. Michael A. Fortune, June 1998.

NESDIS 91 Aliasing of Satellite Altimeter Data in Exact-Repeat Sampling Mode: Analytic Formulas for the Mid-Point Grid. Chang-Kou Tai, March 1999.

NESDIS 92 Calibration of the Advanced Microwave Sounding Unit-A Radiometers for NOAA-L and NOAA-M. Tsan Mo, May 1999.

NESDIS 93 GOES Imager and Sounder Calibration, Scaling, and Image Quality. Donald W. Hillger, June 1999.

NESDIS 94 MSU Antenna Pattern Data. Tsan Mo, Thomas J. Kleespies, and J. Philip Green, March 2000.

NESDIS 95 Preliminary Findings from the Geostationary Interferometer Observing System Simulation Experiments (OSSE). Bob Aune, Paul Menzel, Jonathan Thom, Gail Bayler, Allen Huang, and Paolo Antonelli, June 2000.

NESDIS 96 Hydrography of the Ross Sea Continental Shelf During the Roaverrs, NBP96-06, Cruise December 1996 - January 1997. Michael L. Van Woert, David Pryor, Eric Quiroz, Richard Slonaker, and William Stone, September 2000.

NESDIS 97 Hydrography of the Ross Sea Continental Shelf During the Roaverrs, NBP97-09, Cruise December 1997 - January 1998. Michael L. Van Woert, Lou Gordon, Jackie Grebmeier, Randal Holmbeck, Thomas Henderson, and William F. Van Woert, September 2000.

NESDIS 98 NOAA-L and NOAA-M AMSU-A Antenna Pattern Corrections. Tsan Mo, August 2000.

NESDIS 99 The Use of Water Vapor for Detecting Environments that Lead to Convectively Produced Heavy Precipitation and Flash Floods. Rod Scofield, Gilberto Vicente, and Mike Hodges, September 2000.

NESDIS 100 The Resolving Power of a Single Exact-Repeat Altimetric Satellite or a Coordinated Constellation of Satellites: The Definitive Answer and Data Compression. Chang-Kou Tai, April 2001.

NESDIS 101 Evolution of the Weather Satellite Program in the U.S. Department of Commerce - A Brief Outline. P. Krishna Rao, July 2001.

NESDIS 102 NOAA Operational Sounding Products From Advanced-TOVS Polar Orbiting Environmental Satellites. Anthony L. Reale, August 2001.

NESDIS 103 GOES-11 Imager and Sounder Radiance and Product Validations for the GOES-11 Science Test. Jaime M. Daniels and Timothy J. Schmit, August 2001.

NESDIS 104 Summary of the NOAA/NESDIS Workshop on Development of a Coordinated Coral Reef Research and Monitoring Program. Jill E. Meyer and H. Lee Dantzler, August 2001.

NOAA SCIENTIFIC AND TECHNICAL PUBLICATIONS

The National Oceanic and Atmospheric Administration was established as part of the Department of Commerce on October 3, 1970. The mission responsibilities of NOAA are to assess the socioeconomic impact of natural and technological changes in the environment and to monitor and predict the state of the solid Earth, the oceans and their living resources, the atmosphere, and the space environment of the Earth.

The major components of NOAA regularly produce various types of scientific and technical information in the following types of publications:

PROFESSIONAL PAPERS - Important definitive research results, major techniques, and special investigations.

CONTRACT AND GRANT REPORTS - Reports prepared by contractors or grantees under NOAA sponsorship.

ATLAS - Presentation of analyzed data generally in the form of maps showing distribution of rainfall, chemical and physical conditions of oceans and atmosphere, distribution of fishes and marine mammals, ionospheric conditions, etc.

TECHNICAL SERVICE PUBLICATIONS - Reports containing data, observations, instructions, etc. A partial listing includes data serials; prediction and outlook periodicals; technical manuals, training papers, planning reports, and information serials; and miscellaneous technical publications.

TECHNICAL REPORTS - Journal quality with extensive details, mathematical developments, or data listings.

TECHNICAL MEMORANDUMS - Reports of preliminary, partial, or negative research or technology results, interim instructions, and the like.

U.S. DEPARTMENT OF COMMERCE
National Oceanic and Atmospheric Administration
National Environmental Satellite, Data, and Information Service
Washington, D.C. 20233